

$B \rightarrow \pi \ell^+ \ell^-$ decays revisited in the standard model

Zuo-Hong Li ^{a*}, Zong-Guo Si ^{b†}, Ying Wang^{b‡} and Nan Zhu ^{a§}

^a *Department of Physics, Yantai University, Yantai, 264005, P.R.China*

^b *Department of Physics, Shandong University, Jinan, 25100, P. R. China*

(Dated: July 30, 2018)

Abstract

A new estimate is presented of the dileptonic B decays $B \rightarrow \pi \ell^+ \ell^-$ ($\ell = e, \mu, \tau$) in naive factorization within the standard-model (SM) framework. Using a combination of several approaches, we investigate the behavior of the $B \rightarrow \pi$ form factors in the entire region of the momentum transfer squared q^2 . For the vector and scalar form factors, we employ the light cone sum rule (LCSR) with a chiral current correlator to estimate, at twist-2 next-to-leading order (NLO) accuracy, their shapes in small and intermediate kinematical region. Then a simultaneous fit to a Bourrely-Caprini-Lellouch (BCL) parametrization is performed of the sum rule predictions and the corresponding lattice QCD (LQCD) results available at some high q^2 's. The same approach is applied for the tensor form factor, except that at large q^2 we use as input the LQCD data on the corresponding $B \rightarrow K$ form factor in combination with a $SU_F(3)$ symmetry breaking ansatz. Employing the fitted BCL parameterizations, we evaluate, as an illustrative example, several of the observables of the charged decay modes $B^- \rightarrow \pi^- \ell^+ \ell^-$, including the dilepton invariant mass distribution and branching ratio. For the dielectron and dimuon modes, the branching ratios are estimated at $\mathcal{B}(B^- \rightarrow \pi^- e^+ e^-) = (2.263_{-0.192}^{+0.227}) \times 10^{-8}$ and $\mathcal{B}(B^- \rightarrow \pi^- \mu^+ \mu^-) = (2.259_{-0.191}^{+0.226}) \times 10^{-8}$. The latter shows an excellent agreement with the recent experimental measurement at LHCb and hence puts a stringent constraint on the contribution from possible new physics. We arrive at, for the ditau mode, $\mathcal{B}(B^- \rightarrow \pi^- \tau^+ \tau^-) = (1.017_{-0.139}^{+0.118}) \times 10^{-8}$, which is one order of magnitude larger than the existing theoretical predictions.

* lizh@ytu.edu.cn

† zgsi@sdu.edu.cn

‡ wang_y@mail.sdu.edu.cn

§ zhunan426@126.com

I. INTRODUCTION

Recently, a discovery of the rare decay $B^+ \rightarrow \pi^+\mu^+\mu^-$ has been reported using a pp collision data sample, corresponding to integrated luminosity of $1.0fb^{-1}$, collected with the LHCb experiment at the Large Hadron Collider [1]. The branching ratio was measured at $\mathcal{B}(B^+ \rightarrow \pi^+\mu^+\mu^-) = (2.3 \pm 0.6(stat.) \pm 0.1(syst.)) \times 10^{-8}$ with 5.2σ significance. It is the first time flavor-changing neutral current (FCNC) $b \rightarrow d\ell^+\ell^-$ transitions have been observed. As data accumulates, more and more attention would be paid to this aspect.

As is known to all, dileptonic decays of B -meson induced by FCNC $b \rightarrow s(d)$ transitions serve as an important avenue to test the standard model (SM) and search for physics beyond it. The transition matrix elements contain terms proportional respectively to the products of the Cabibbo-Kobayashi-Maskawa (CKM) matrix elements, $V_{tb}V_{ts}^*$, $V_{cb}V_{cs}^*$ and $V_{ub}V_{us}^*$. Using unitarity of the CKM matrix and neglecting the smaller $V_{ub}V_{us}^*$ term in comparison to $V_{tb}V_{ts}^*$ and $V_{cb}V_{cs}^*$, only one independent CKM factor $V_{tb}V_{ts}^*$ is involved in the $b \rightarrow s\ell^+\ell^-$ transitions in this approximation. In contrast, the CKM factors $V_{tb}V_{td}^*$, $V_{cb}V_{cd}^*$ and $V_{ub}V_{ud}^*$ are at the same order of magnitude. Consequently, for the $b \rightarrow d$ modes there could be a considerable CP asymmetry, but meanwhile they are suppressed by a factor of about $|V_{td}/V_{ts}|$ with respect to the $b \rightarrow s$ transitions. This indicates that the $b \rightarrow d$ dileptonic transitions can be complementary to the $b \rightarrow s$ ones in probing new physics.

Some theoretical effort has been devoted to research for the exclusive decays $B \rightarrow \pi\ell^+\ell^-$ ($\ell = e, \mu, \tau$) within [2–7] and beyond [8–10] the SM. The naive factorization approach is extensively adopted in these studies and the resulting SM branching ratios for the dimuonic modes [3–6] turn out to be consistent with the experimental data. Very recently, in the limits of the heavy quark mass and large recoil energy, corresponding to small dilepton mass squared q^2 , a detailed analysis [7] appeared within the framework of QCD factorization (QCDF) [11–17], which modifies naive factorization by including the factorizable hard-gluon corrections to weak vertex and non-factorizable hard spectator scattering contributions, an important potential source of CP-asymmetry, W -weak annihilation, being identified. A partial understanding is also achievable of the nonlocal corrections due to soft-gluon emission and hadronic resonance which could not be covered by QCDF, using the QCD light cone sum rule (LCSR) approach applied for the $B \rightarrow K$ dileptonic modes [18]. However, the largest uncertainty in calculating the decay rates and widths originates from

the $B \rightarrow \pi$ transition form factors $f_+^{B \rightarrow \pi}(q^2)$, $f_0^{B \rightarrow \pi}(q^2)$ and $f_T^{B \rightarrow \pi}(q^2)$ (conventionally called vector, scalar and tensor form factors, respectively), of which, the first two and $f_T^{B \rightarrow \pi}(q^2)$ parameterize, respectively, the matrix elements of the vector and the tensor currents as

$$\begin{aligned} \langle \pi(p) | \bar{d} \gamma_\mu b | B(p+q) \rangle &= (2p+q)_\mu f_+^{B \rightarrow \pi}(q^2) + \frac{m_B^2 - m_\pi^2}{q^2} q_\mu (f_0^{B \rightarrow \pi}(q^2) - f_+^{B \rightarrow \pi}(q^2)), \\ \langle \pi(p) | \bar{d} \sigma_{\mu\nu} q^\nu b | B(p+q) \rangle &= i \left((2p+q)_\mu q^2 - (m_B^2 - m_\pi^2) q_\mu \right) \frac{f_T^{B \rightarrow \pi}(q^2)}{m_B + m_\pi}, \end{aligned} \quad (1)$$

where the 4-momentum assignment is specified in brackets, and m_B (m_π) denotes the B (π) meson mass. Leaving aside potential uncertainties with the existing QCD approaches to form factors for heavy-to-light B decays, the key problem is that none of them is applicable in the entire q^2 region. Whereas lattice QCD (LQCD) simulation, as a rigorous approach, could make prediction at large q^2 , QCD LCSR [19, 20] and perturbative QCD (pQCD) [21] approaches are applicable for low and intermediate q^2 . In [3] the LCSR computations presented by [22] were extrapolated to the high q^2 region by using the B^* -dominance assumption, to make an estimate for $B \rightarrow \pi \ell^+ \ell^-$. The same was done in pQCD approach [4]. To enhance prediction accuracy for the $B \rightarrow \pi$ form factors in the whole physical region, a quasi-model-independent approach [5] has recently been suggested, in which use was made of available experimental measurements as well as theoretical predictions from LQCD simulation and other scenarios. For example, the shape of the vector form factor was extracted from the experimental data on the $B \rightarrow \pi \ell \nu_\ell$ semileptonic decays; for determination of q^2 -behavior of the tensor form factor, the constraints were utilized from the LQCD data on the corresponding $B \rightarrow K$ form factor combined with an ansatz on $SU_F(3)$ symmetry breaking, and the heavy quark symmetry in the large recoil limit. However, the vector form factor obtained therein by data-fitting is based on use of the result from the CKM unitarity fits [23], $|V_{ub}| = (3.51_{-0.14}^{+0.15}) \times 10^{-3}$, which is incompatible with inclusive determinations. To say at least, even if it reflects the true value of $|V_{ub}|$, the form factor shape extracted experimentally requires a dynamical interpretation.

Given the fact that LCSR approach has exhibited a stronger predictive power in its applications to numerous exclusive processes, and could be substantially complementary to LQCD simulation in the aspect of predicting the form factors, in this study we attempt to combine the LCSR calculations with the available LQCD results and the analyticity of the form factors, to reevaluate $f_+^{B \rightarrow \pi}(q^2)$, $f_T^{B \rightarrow \pi}(q^2)$ and $f_0^{B \rightarrow \pi}(q^2)$, and then in naive factorization explore the $B \rightarrow \pi \ell^+ \ell^-$ decays and make comparison with the recent study of [5].

Calculations of the form factors in question have already been undertaken many times within the LCSR framework. One can be referred to [24, 25] for a recent application of this approach. At QCD next-leading-order (NLO) level for twist-2 and -3, the first complete study on these form factors was put forward in [22], with the pole mass for the underlying heavy quark in light-cone operator product expansion (OPE) calculation of the correlation functions. To the same accuracy, instead using the $\overline{\text{MS}}$ mass the authors of [26] furnished an updated computation, with which $|V_{ub}|$ was extracted from the the BarBar data [27]. Here we would like to take an alternative version suggested in [20, 24, 28], in which a certain chiral current correlator is so chosen that the twist-3 and -5 components of the pionic light-cone distribution amplitudes (DAs) do not contribute and thus the resulting sum rules receive less pollution than in the case of the standard correlation functions. It should be added that the calculations with LCSR involve soft-overlap as well as hard-exchange components, and the former plays a predominant role. It forms a striking contrast to the situation when applying pQCD approach [21], in which hard-exchange dominates.

This paper is organized as follows. The following section encompasses a concise derivation of the LCSRs for the $B \rightarrow \pi$ vector, scalar and tensor form factors and numerical analysis. In section 3 we turn to the discussion about the shapes of the form factors in the whole kinematically accessible region. In section 4, we apply our findings to estimate the decay rates and branching ratios for the $B \rightarrow \pi$ dileptonic decays, including the ditau modes, and also the partial branching ratios in some chosen q^2 bins. The final section is devoted to a concluding remark.

II. LCSR CALCULATION OF THE $B \rightarrow \pi \ell^+ \ell^-$ FORM FACTORS

Essentially, LCSR approach is through the twist expansion of, say, a vacuum-to-pion correlation function in the small light-cone distance $x^2 \approx 0$ and in the strong coupling α_s , which works effectively out some of the problems with the short distance ($x \approx 0$) expansion in terms of vacuum condensates. To validate the light-cone OPE, the higher-twist terms are required to be suppressed. In the heavy quark expansion [29], it is seen readily that higher-twist contributions increase with q^2 so that for larger q^2 the twist hierarchy breaks down. The accessible kinematical region can be approximately fixed at $0 \leq q^2 \leq 12 - 14 \text{ GeV}^2$. In the ensuing LCSR calculation, we will restrict ourself to the interval $0 \leq q^2 \leq 12 \text{ GeV}^2$, to

ensure the validity of results.

A. NLO QCD calculation

We employ the following vacuum-to-pion correlation functions to achieve a LCSR estimate of the $B \rightarrow \pi \ell^+ \ell^-$ form factors,

$$\begin{aligned} F_\mu(p, q) &= i \int d^4x e^{iq \cdot x} \langle \pi(p) | T \{ \bar{d}(x) \gamma_\mu (1 + \gamma_5) b(x), m_b \bar{b}(0) i(1 + \gamma_5) u(0) \} | 0 \rangle \\ &= F(q^2, (p+q)^2) p_\mu + \bar{F}(q^2, (p+q)^2) q_\mu, \end{aligned} \quad (2)$$

$$\begin{aligned} \tilde{F}_\mu(p, q) &= i \int d^4x e^{iq \cdot x} \langle \pi(p) | T \{ \bar{d}(x) i \sigma_{\mu\nu} q^\nu (1 + \gamma_5) b(x), m_b \bar{b}(0) i(1 - \gamma_5) u(0) \} | 0 \rangle \\ &= \tilde{F}(q^2, (p+q)^2) [q_\mu (q \cdot p) - p_\mu q^2], \end{aligned} \quad (3)$$

with m_b being the b quark mass, and take the chiral limit $m_\pi = 0$ for the pion mass throughout the derivation. Note that a T-product of chiral currents, which keeps the hadronic contribution to the correlation function positive definite, is substituted for the corresponding one adopted in the standard approach. In a large space-like momentum region $(p+q)^2 \ll 0$ and the effective q^2 interval, the correlation functions can be expanded in the small light-cone distance $x^2 \approx 0$, and however, the operator replacements result in an explicitly different OPE, in which, especially, no twist-3 and -5 component is involved, as aforementioned and seen below. As a result, the invariant functions $F(q^2, (p+q)^2)$, $\bar{F}(q^2, (p+q)^2)$ and $\tilde{F}(q^2, (p+q)^2)$, which have the generic expansion in α_s ,

$$H^{QCD}(q^2, (p+q)^2) = H_0^{QCD}(q^2, (p+q)^2) + \frac{\alpha_s C_F}{4\pi} H_1^{QCD}(q^2, (p+q)^2) + \dots \quad (4)$$

are made accessible at twist-5 level with the existing findings of the twist-2 and -4 DAs. The resulting difference in hadronic expression is that there are the additional terms due to the complete set of scalar (0^+) B meson states. However, this causes no problem, because they are located far away from the lowest pseudoscalar state and therefore their contributions can safely be absorbed in a dispersion integral.

According to the standard procedure of sum rule calculation, the form factors in question are accessible. Assuming the quark-hadron duality and matching the OPE form of the correlation function (2)

$$F_\mu^{QCD}(p, q) = F^{QCD}(q^2, (p+q)^2) p_\mu + \bar{F}^{QCD}(q^2, (p+q)^2) q_\mu, \quad (5)$$

with the corresponding hadronic one, which follows from inserting the complete sets of both the pseudoscalar and scalar states between the currents of (2) and then isolating the pole contribution from the lowest B meson, we obtain

$$\frac{2m_B^2 f_B f_+^{B \rightarrow \pi}(q^2)}{m_B^2 - (p+q)^2} = \frac{1}{\pi} \int_{m_b^2}^{s_0} \frac{\text{Im} F^{QCD}(q^2, s)}{s - (p+q)^2} ds, \quad (6)$$

$$\frac{m_B^4 f_B}{q^2(m_B^2 - (p+q)^2)} \left(f_0^{B \rightarrow \pi}(q^2) - \frac{m_B^2 - q^2}{m_B^2} f_+^{B \rightarrow \pi}(q^2) \right) = \frac{1}{\pi} \int_{m_b^2}^{s_0} \frac{\text{Im} \bar{F}^{QCD}(q^2, s)}{s - (p+q)^2} ds, \quad (7)$$

with f_B being the decay constant defined as $m_B^2 f_B = \langle B | m_b \bar{b} i \gamma_5 u | 0 \rangle$, s_0 an effective threshold to be determined and $f_0^{B \rightarrow \pi}(0) = f_+^{B \rightarrow \pi}(0)$. On the Borel transformation $(p+q)^2 \rightarrow M^2$ for the above equations, we have the sum rules for the vector and the scalar form factors:

$$f_+^{B \rightarrow \pi}(q^2) = \frac{1}{2m_B^2 f_B} e^{m_B^2/M^2} F(q^2, M^2, s_0), \quad (8)$$

$$f_0^{B \rightarrow \pi}(q^2) = \frac{m_B^2 - q^2}{m_B^2} f_+^{B \rightarrow \pi}(q^2) + \frac{q^2}{m_B^4 f_B} e^{m_B^2/M^2} \bar{F}(q^2, M^2, s_0), \quad (9)$$

where the functions $F(q^2, M^2, s_0)$ and $\bar{F}(q^2, M^2, s_0)$ have the following form,

$$\begin{aligned} H(q^2, M^2, s_0) &= \frac{1}{\pi} \int_{m_b^2}^{s_0} ds e^{-s/M^2} \text{Im} H^{QCD}(q^2, s) \\ &= H_0(q^2, M^2, s_0) + \frac{\alpha_s C_F}{4\pi} H_1(q^2, M^2, s_0) + \dots \end{aligned} \quad (10)$$

For the correlation function (3), a similar manipulation results in the sum rule for the tensor form factor,

$$f_T^{B \rightarrow \pi}(q^2) = \frac{1}{2m_B f_B} e^{m_B^2/M^2} \tilde{F}(q^2, M^2, s_0), \quad (11)$$

with $\tilde{F}(q^2, M^2, s_0)$ being defined the same as $F(q^2, M^2, s_0)$ and $\bar{F}(q^2, M^2, s_0)$.

We are to do the OPE calculation at one-loop level for twist-2. The LO functions, $F_0(q^2, M^2, s_0)$, $\bar{F}_0(q^2, M^2, s_0)$ and $\tilde{F}_0(q^2, M^2, s_0)$, are easy to get, by contracting the b quark fields of (2) and (3) to the free quark propagator plus a correction term from one-gluon emission and using the definition of the pion DAs [30–32]. Then it becomes clear that the twist-3 and-5 contributions vanish due to the Dirac structures. The results read,

$$F_0(q^2, M^2, s_0) = 2m_b^2 f_\pi \int_{u_0}^1 du e^{-\frac{m_b^2 - q^2 u}{u M^2}} \left\{ \frac{\varphi_\pi(u)}{u} + \frac{1}{m_b^2 - q^2} \left(-\frac{m_b^2 u}{4(m_b^2 - q^2)} \frac{d^2 \phi_{4\pi}(u)}{du^2} \right) \right\}$$

$$+ u\psi_{4\pi}(u) + \int_0^u dv\psi_{4\pi}(v) - \frac{d}{du}J_{4\pi}(u) \Big\}, \quad (12)$$

$$\bar{F}_0(q^2, M^2, s_0) = 2m_b^2 f_\pi \int_{u_0}^1 du e^{-\frac{m_b^2 - q^2 \bar{u}}{uM^2}} \frac{1}{m_b^2 - q^2} \psi_{4\pi}(u), \quad (13)$$

$$\begin{aligned} \tilde{F}_0(q^2, M^2, s_0) &= 2m_b f_\pi \int_{u_0}^1 du e^{-\frac{m_b^2 - q^2 \bar{u}}{uM^2}} \left\{ \frac{\varphi_\pi(u)}{u} + \frac{1}{m_b^2 - q^2} \left(\frac{1}{4} \frac{d\phi_{4\pi}(u)}{du} \right. \right. \\ &\quad \left. \left. - \frac{m_b^2 u}{2(m_b^2 - q^2)} \frac{d^2\phi_{4\pi}(u)}{du^2} - \frac{d}{du} \tilde{J}_{4\pi}(u) \right) \right\}. \end{aligned} \quad (14)$$

In the above, $\bar{u} = 1 - u$, $u_0 = (m_b^2 - q^2)/(s_0 - q^2)$, f_π indicates the pionic decay constant, $J_{4\pi}(u)$ and $\tilde{J}_{4\pi}(u)$ are two integral functions:

$$\begin{aligned} J_{4\pi}(u) &= \int_0^u d\alpha_1 \int_{\frac{u-\alpha_1}{1-\alpha_1}}^1 \frac{dv}{v} \left[2\Psi_{4\pi}(\alpha_i) + 2\tilde{\Psi}_{4\pi}(\alpha_i) \right. \\ &\quad \left. - \Phi_{4\pi}(\alpha_i) - \tilde{\Phi}_{4\pi}(\alpha_i) \right] \Big|_{\substack{\alpha_2=1-\alpha_1-\alpha_3 \\ \alpha_3=(u-\alpha_1)/v}}, \end{aligned} \quad (15)$$

$$\begin{aligned} \tilde{J}_{4\pi}(u) &= \int_0^u d\alpha_1 \int_{\frac{u-\alpha_1}{1-\alpha_1}}^1 \frac{dv}{v} \left[2\Psi_{4\pi}(\alpha_i) + 2(1-2v)\tilde{\Psi}_{4\pi}(\alpha_i) \right. \\ &\quad \left. - (1-2v)\Phi_{4\pi}(\alpha_i) - \tilde{\Phi}_{4\pi}(\alpha_i) \right] \Big|_{\substack{\alpha_2=1-\alpha_1-\alpha_3 \\ \alpha_3=(u-\alpha_1)/v}}; \end{aligned} \quad (16)$$

$\varphi_\pi(u)$ denotes the leading twist-2 DA, while $\phi_{4\pi}(u)$, $\psi_{4\pi}(u)$ and those functions included in the integrands of (15) and (16) have all twist-4.

By substituting (12), (13) and (14), respectively, into (8), (9) and (11), the resulting sum rules for $f_+^{B \rightarrow \pi}(q^2)$, $f_0^{B \rightarrow \pi}(q^2)$ and $f_T^{B \rightarrow \pi}(q^2)$ respect, up to the higher twist and QCD radiative corrections, the following relations which are similar to the observations in the limits of heavy quark mass and large recoil energy [33, 34]:

$$f_0^{B \rightarrow \pi}(q^2) = \frac{m_B^2 - q^2}{m_B^2} f_+^{B \rightarrow \pi}(q^2), \quad (17)$$

$$\begin{aligned} f_T^{B \rightarrow \pi}(q^2) &= \frac{m_B}{m_b} f_+^{B \rightarrow \pi}(q^2) \\ &= \frac{m_B^3}{m_b} \left(\frac{f_+^{B \rightarrow \pi}(q^2) - f_0^{B \rightarrow \pi}(q^2)}{q^2} \right), \end{aligned} \quad (18)$$

so that in such an approximation only one independent form factor is necessary for describing the non-perturbative QCD dynamics involved in the $B \rightarrow \pi$ transitions. In effect, in the case of using the standard correlation functions the same relations hold numerically approximately, despite not explicitly appearing. All these provide an important validity check of the present approach.

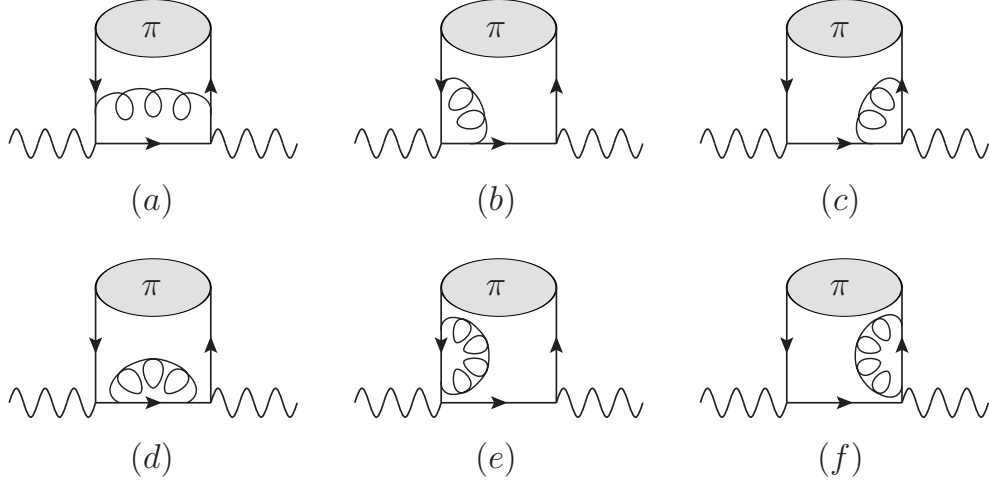


FIG. 1: One-loop Feynman diagrams contributing to the correction functions.

For getting the NLO corrections, $F_1(q^2, M^2, s_0)$, $\bar{F}_1(q^2, M^2, s_0)$ and $\tilde{F}_1(q^2, M^2, s_0)$, we turn to calculation of the invariant functions $F_1^{QCD}(q^2, (p+q)^2)$, $\bar{F}_1^{QCD}(q^2, (p+q)^2)$ and $\tilde{F}_1^{QCD}(q^2, (p+q)^2)$ (with the relevant Feynman diagrams plotted in Fig.1). Apparently they can be expressed uniformly as a convolution of the corresponding hard scattering amplitudes with the twist-2 DA: for example,

$$F_1^{QCD}(q^2, (p+q)^2) = -f_\pi \int_0^1 du T_1^H(q^2, (p+q)^2, u) \varphi_\pi(u), \quad (19)$$

and hence our task boils down to computing the scattering functions $T_1^H(q^2, (p+q)^2, u)$, $\bar{T}_1^H(q^2, (p+q)^2, u)$ and $\tilde{T}_1^H(q^2, (p+q)^2, u)$.

To this end, we take the Feynman gauge, and adopt the dimensional regularization and the $\overline{\text{MS}}$ mass \bar{m}_b for the underlying b quark. In fact, the same prescription has been employed to investigate the QCD radiative correction to the vector form factor at $q^2 = 0$ in [24], where a detailed derivation of $F_1^{QCD}(q^2 = 0, (p+q)^2)$ is presented. Using the technic described therein, the invariant functions in question could be worked out. In what follows, we just highlight the key points and main results in the NLO calculation.

At first we concentrate on a discussion of $F_1^{QCD}(q^2, (p+q)^2)$. A straightforward calculation shows that there are both ultraviolet (UV) and infrared (IR) divergences to deal with in $T_1^H(q^2, (p+q)^2, u)$. By performing the mass renormalization, $m_b \rightarrow Z_m \bar{m}_b$ with Z_m being the familiar renormalization constant, the UV divergence, as expected, is precisely offset by the one appearing in the resulting LO term, leading to an UV finite hard scattering amplitude written down in terms of the $\overline{\text{MS}}$ mass that we denote by m_b hereafter, unless otherwise

stated. As for the IR divergence term, it can be eliminated by replacing the bare quantity $\varphi_\pi(u)$ of (19) with a renormalized DA $\varphi_\pi(u, \mu)$. As a result, we are left with the invariant function $F_1^{QCD}(q^2, (p+q)^2)$ expressed by the convolution of $\varphi_\pi(u, \mu)$ with a scale-dependent NLO hard kernel $T_1^H(\eta_1, \eta_2, u, \mu)$ obtained as following,

$$\begin{aligned}
T_1^H(\eta_1, \eta_2, u, \mu) &= 4 \left(\frac{1}{1-\eta} + \frac{\eta_2-1}{u(\eta_2-\eta_1)^2} \right) L(\eta_1) + 4 \left(\frac{1}{1-\eta} - \frac{1-\eta_1}{\bar{u}(\eta_2-\eta_1)^2} \right) L(\eta_2) \\
&- 4 \left(\frac{2}{1-\eta} + \frac{\eta_2-1+u(\eta_1-\eta_2)}{u\bar{u}(\eta_1-\eta_2)^2} \right) L(\eta) \\
&- \frac{4}{\eta_2} \left(\frac{\eta_2-1}{\eta-1} - \frac{\eta_2-1}{\bar{u}(\eta_2-\eta_1)} \right) \ln(1-\eta_2) - \frac{2}{\eta_2} \left(\frac{\eta_2-2}{\eta} - \frac{\eta_2}{\eta^2} + \frac{2(\eta_2-1)}{\bar{u}(\eta_2-\eta_1)} \right) \\
&\times \ln(1-\eta) - \frac{2(\eta+1)}{(\eta-1)^2} \left(3\ln\frac{m_b^2}{\mu^2} - \frac{3\eta+1}{\eta} \right), \tag{20}
\end{aligned}$$

where $\eta_1 = q^2/m_b^2$, $\eta_2 = (p+q)^2/m_b^2$, $\eta = \eta_1 + u(\eta_2 - \eta_1)$, and $L(x)$ indicates a linear combination of the form:

$$L(x) = \text{Li}_2(x) + \ln^2(1-x) + \ln(1-x) \left(\ln\frac{m_b^2}{\mu^2} - 1 \right),$$

with the dilogarithm $\text{Li}_2(x) = -\int_0^x dx \frac{\ln(1-x)}{x}$. It should be understood that here and hereafter the factorization scale is specified to be equal to the renormalization one. Putting everything together yields the desired result,

$$F_1(q^2, M^2, s_0) = -\frac{f_\pi}{\pi} \int_{m_b^2}^{s_0} ds e^{-s/M^2} \int_0^1 du \text{Im} T_1^H(\eta_1, \eta_2, u, \mu) \varphi_\pi(u, \mu), \tag{21}$$

with $\eta_2 = s/m_b^2 > 1$ (in the following the same should be understood when taking imaginary part for a hard kernel), and

$$\begin{aligned}
\frac{1}{2\pi} \text{Im} T_1^H(\eta_1, \eta_2, u, \mu) &= \delta(1-\eta) \left[6 - 3\ln\frac{m_b^2}{\mu^2} - \frac{7}{3}\pi^2 + 2\text{Li}_2(\eta_1) - 2\text{Li}_2(1-\eta_2) \right. \\
&+ 2(\ln^2(1-\eta_1) + \ln^2(\eta_2-1)) - 2 \left(\ln\eta_2 + \frac{1-\eta_2}{\eta_2} \right) \ln(\eta_2-1) \\
&- 2\ln((1-\eta_1)(\eta_2-1)) \left(1 - \ln\frac{m_b^2}{\mu^2} \right) - 2 \left(4 - 3\ln\frac{m_b^2}{\mu^2} \right) \left(1 + \frac{d}{d\eta} \right) \Big] \\
&+ \theta(\eta-1) \left[\frac{4}{\eta-1} \Big|_+ \left(\ln\left(\frac{(\eta-1)^2 m_b^2}{\eta \mu^2} \right) - 1 \right) - \frac{2}{\eta-1} \Big|_+ \left(\ln\left(\frac{(\eta_2-1)^2 m_b^2}{\eta_2 \mu^2} \right) - \frac{1}{\eta_2} \right) \right. \\
&- 2 \frac{1-\eta_1}{(\eta_2-\eta_1)(\eta_2-\eta)} \left(\ln\left(\frac{(\eta_2-1)^2 m_b^2}{\eta_2 \mu^2} \right) - 1 \right) + \frac{1}{\eta} \left(\frac{1}{\eta} + \frac{2}{\eta_2} - 1 \right) \\
&\left. + 2 \frac{1+\eta-\eta_1-\eta_2}{(\eta_1-\eta)(\eta_2-\eta)} \left(\ln\left(\frac{(\eta-1)^2 m_b^2}{\eta \mu^2} \right) - 1 \right) \right]
\end{aligned}$$

$$\begin{aligned}
& + \theta(1 - \eta) \left[2 \left(\ln \frac{\eta_2}{(\eta_2 - 1)^2} + \frac{1}{\eta_2} - \ln \frac{m_b^2}{\mu^2} \right) \frac{1}{\eta - 1} \Big|_+ \right. \\
& \left. - 2 \frac{1 - \eta_1}{(\eta_1 - \eta_2)(\eta_2 - \eta)} \left(\ln \frac{\eta_2}{(\eta_2 - 1)^2} + 1 - \ln \frac{m_b^2}{\mu^2} \right) - 2 \frac{1}{\eta_2 - \eta} \frac{1 - \eta_2}{\eta_2} \right]. \tag{22}
\end{aligned}$$

Note the operation,

$$\frac{F(\eta)}{1 - \eta} \Big|_+ = \frac{F(\eta) - F(1)}{1 - \eta}, \tag{23}$$

is introduced to avert the redundant IR divergences generated by taking the imaginary part. Finally, using the known $F_1(q^2, M^2, s_0)$ and $F_0(q^2, M^2, s_0)$ we achieve the function $F(q^2, M^2, s_0)$ with $\mathcal{O}(\alpha_s)$ accuracy, where the changes with scale compensate each other of the hard kernel and the twist-2 DA, having QCD factorization observed.

Contrasted with the above situation, neither UV nor IR divergences appear in the calculation of $\overline{F}_1^{QCD}(q^2, (p + q)^2)$. The NLO hard kernel reads as,

$$\begin{aligned}
\overline{T}_1^H(\eta_1, \eta_2, u) &= 2 \left[\frac{\eta_1^2 - \eta_1 \eta_2 - (1 - \eta_1)(\eta_2 - \eta_1) \ln(1 - \eta_1)}{\eta_1^2(1 - \eta)} - \frac{(1 - \eta_1)(\eta_1 + \eta_2) \ln(1 - \eta_1)}{u \eta_1^2(\eta_2 - \eta_1)} \right. \\
& \left. + 2 \frac{(\eta_2 - 1) \ln(1 - \eta_2)}{\bar{u} \eta_2(\eta_2 - \eta_1)} - \frac{(\eta - 1)(\eta_2 + \eta) \ln(1 - \eta)}{u \bar{u}(\eta_2 - \eta_1) \eta^2} - \frac{\eta_2 - \eta_1}{\eta_1 \eta} \right]. \tag{24}
\end{aligned}$$

From this, we derive the NLO function $\overline{F}_1(q^2, M^2, s_0)$,

$$\overline{F}_1(q^2, M^2, s_0) = -\frac{f_\pi}{\pi} \int_{m_b^2}^{s_0} ds e^{-s/M^2} \int_0^1 du \text{Im} \overline{T}_1^H(\eta_1, \eta_2, u) \varphi_\pi(u, \mu), \tag{25}$$

$$\begin{aligned}
\frac{1}{2\pi} \text{Im} \overline{T}_1^H(\eta_1, \eta_2, u) &= \delta(1 - \eta) \left[1 - \frac{\eta_2}{\eta_1} - \frac{(\eta_1 - 1)(\eta_1 - \eta_2) \ln(1 - \eta_1)}{\eta_1^2} \right] \\
& + \theta(\eta - 1) \left[\frac{2(\eta_2 - 1)}{\eta_2(\eta_2 - \eta)} - \frac{(\eta - 1)(\eta_2 + \eta)}{u \bar{u} \eta^2(\eta_2 - \eta_1)} \right] \\
& + \theta(1 - \eta) \frac{2(\eta_2 - 1)}{\eta_2(\eta_2 - \eta)}. \tag{26}
\end{aligned}$$

As a consequence, the complete function $\overline{F}(q^2, M^2, s_0)$ has a QCD factorized form, in which the hard kernel is scale-independent.

To proceed, we embark upon discussing the case of the tensor form factor. In dealing with the hard amplitude $\widetilde{T}_1^H(q^2, (p + q)^2, u)$, we find that in addition to an IR divergence which can be removed as in the case of $T_1^H(q^2, (p + q)^2, u)$, there is an UV divergence left after the mass renormalization. It is not surprising because the effective weak operator of the related correlation function is a combination of the tensor and the pseudo-tensor operators, which

require a renormalization, as compared with the vector (axial-vector) operator. On taking this point into account, the divergence, indeed, could be canceled out by that entering the renormalization constant of the effective current, which, from another perspective, provides a confirmation of the calculation. We have the hard kernel,

$$\begin{aligned}
\tilde{T}_1^H(\eta_1, \eta_2, u, \mu) = & \frac{4}{m_b} \left[\left(\frac{1}{1-\eta} + \frac{\eta_2-1}{u(\eta_2-\eta_1)^2} \right) L(\eta_1) \right. \\
& + \left(\frac{1}{1-\eta} - \frac{1-\eta_1}{\bar{u}(\eta_2-\eta_1)^2} \right) L(\eta_2) + \left(\frac{1-\eta_2-u(\eta_1-\eta_2)}{u\bar{u}(\eta_1-\eta_2)^2} - \frac{2}{1-\eta} \right) L(\eta) \\
& + \left(\frac{1-\eta_1}{u\eta_1(\eta_2-\eta_1)} + \frac{1-\eta_1}{\eta_1(1-\eta)} \right) \ln(1-\eta_1) + \left(\frac{\eta_2-1}{\eta_2(1-\eta)} - \frac{\eta_2-1}{\bar{u}(\eta_2-\eta_1)\eta_2} \right) \ln(1-\eta_2) \\
& - \left(\frac{1}{2\eta^2} - \frac{\eta_2-1}{\bar{u}(\eta_2-\eta_1)\eta_2} + \frac{1-\eta_1}{u\eta_1(\eta_2-\eta_1)} - \frac{2\eta_2+\eta_2\eta_1-2\eta_1}{2\eta_1\eta_2\eta} \right) \ln(1-\eta) \\
& \left. - \left(\frac{1}{2(1-\eta)} + \frac{3}{(1-\eta)^2} \right) \ln \frac{m_b^2}{\mu^2} + \frac{1}{1-\eta} - \frac{1}{2\eta} + \frac{4}{(1-\eta)^2} \right], \tag{27}
\end{aligned}$$

and the imaginary part,

$$\begin{aligned}
\frac{m_b}{4\pi} \text{Im} \tilde{T}_1^H(\eta_1, \eta_2, u, \mu) = & \delta(1-\eta) \left\{ -\frac{7}{6}\pi^2 + 1 + \text{Li}_2(\eta_1) - \text{Li}_2(1-\eta_2) + \ln^2(1-\eta_1) \right. \\
& + \ln^2(\eta_2-1) - \ln((1-\eta_1)(\eta_2-1)) \left(1 - \ln \frac{m_b^2}{\mu^2} \right) + \frac{1-\eta_1}{\eta_1} \ln(1-\eta_1) \\
& \left. - \left(\frac{1-\eta_2}{\eta_2} + \ln \eta_2 \right) \ln(\eta_2-1) - \frac{1}{2} \ln \frac{m_b^2}{\mu^2} + \left(-4 + 3 \ln \frac{m_b^2}{\mu^2} \right) \frac{d}{d\eta} \right\} \\
& + \theta(\eta-1) \left\{ \frac{1-\eta_1}{(\eta_2-\eta_1)(\eta-\eta_2)} \left[\ln \left(\frac{(\eta_2-1)^2 m_b^2}{\eta_2 \mu^2} \right) - 1 \right] \right. \\
& + \frac{1+\eta-\eta_1-\eta_2}{(\eta-\eta_1)(\eta_2-\eta)} \left[\ln \left(\frac{(\eta-1)^2 m_b^2}{\eta \mu^2} \right) - 1 \right] - \left[\ln \left(\frac{(\eta_2-1)^2 m_b^2}{\eta_2 \mu^2} \right) - \frac{1}{\eta_2} \right] \frac{1}{\eta-1} \Big|_+ \\
& + 2 \left[\ln \left(\frac{(\eta-1)^2 m_b^2}{\eta \mu^2} \right) - 1 \right] \frac{1}{\eta-1} \Big|_+ + \frac{\eta_1-1}{\eta_1(\eta-\eta_1)} - \frac{1}{2\eta^2} + \frac{\eta_1\eta_2+2(\eta_2-\eta_1)}{2\eta\eta_1\eta_2} \left. \right\} \\
& + \theta(1-\eta) \left\{ \frac{1-\eta_1}{(\eta_2-\eta_1)(\eta-\eta_2)} \left[\ln \left(\frac{(\eta_2-1)^2 m_b^2}{\eta_2 \mu^2} \right) - 1 \right] \right. \\
& \left. - \left[\ln \left(\frac{(\eta_2-1)^2 m_b^2}{\eta_2 \mu^2} \right) - \frac{1}{\eta_2} \right] \frac{1}{\eta-1} \Big|_+ + \frac{1-\eta_2}{\eta_2(\eta_2-\eta)} \right\}. \tag{28}
\end{aligned}$$

Since the scale dependence of the perturbative kernel including the NLO correction (27) does not cancel out that of $\varphi_\pi(u, \mu)$, we achieve a scale-dependent factorization form for $\tilde{F}(q^2, M^2, s_0)$, with the NLO term,

$$\tilde{F}_1(q^2, M^2, s_0) = -\frac{f_\pi}{\pi} \int_{m_b^2}^{s_0} ds e^{-s/M^2} \int_0^1 du \text{Im} \tilde{T}_1^H(\eta_1, \eta_2, u, \mu) \varphi_\pi(u, \mu). \tag{29}$$

Completing our LCSR calculations of $f_+^{B \rightarrow \pi}(q^2)$, $f_0^{B \rightarrow \pi}(q^2)$ and $f_T^{B \rightarrow \pi}(q^2)$, we associate with (8-11) the obtained LO expressions for $F(q^2, M^2, s_0)$, $\bar{F}(q^2, M^2, s_0)$ and $\tilde{F}(q^2, M^2, s_0)$ and twist-2 NLO corrections.

Lastly, we make a few remarks: (1) Because of the vanishing contribution of the subleading twist-3 components, the twist-4 terms play a subdominant role in the resulting sum rules. They are highly suppressed by the factor of $1/(m_b^2 - q^2)$ with respect to the leading twist-2 ones, in small and intermediate kinematical region, so that the LCSR expressions show a good twist hierarchy and thus are well convergent. (2) Actually, no odd-twist component is involved in the present approach to any order in $\mathcal{O}(\alpha_s)$, as readily verified.

B. Numerical discussion

We proceed to do numerical analysis, starting with choice of input parameters entering the LCSR expressions. Obviously, the leading twist-2 DA, which obeys a conformal expansion in the Gegenbauer polynomials as

$$\varphi_\pi(u, \mu) = 6u\bar{u} \left(1 + \sum_{n=1}^{\infty} a_{2n}^\pi(\mu) C_{2n}^{3/2}(u - \bar{u}) \right), \quad (30)$$

remains the most important source of uncertainty in the sum rule computation. A keen interest is taken in the first two moment parameters $a_2^\pi(\mu)$ and $a_4^\pi(\mu)$, since the Gegenbauer polynomials of higher-degree, which are rapidly oscillating, are usually considered less important from a phenomenological point of view. Given that the existing determinations from some nonperturbative approaches involve a large uncertainty, one has attempted to acquire them by matching theoretical computation of a physical observable, regardless of the higher-moment corrections, with its experimental observation. For example, fitting the LCSR for the pion electromagnetic form factor to the experimental data obtains [27] $a_2^\pi(\mu = 1\text{GeV}) = 0.17 \pm 0.08$ and $a_4^\pi(\mu = 1\text{GeV}) = 0.06 \pm 0.1$. Also, there exists some effort in exploring the higher-moment effects [30, 35–38]. A recent study of $\gamma\gamma^* \rightarrow \pi^0$ form factor [38] reveals that higher-moment terms do indeed play a minor role and gives the three sets of fitted parameters at $\mu = 1$ GeV:

$$\begin{aligned} \text{(I)} \quad & a_2^\pi = 0.130, a_4^\pi = 0.244, a_6^\pi = 0.179, a_8^\pi = 0.141, a_{10}^\pi = 0.116, a_{12}^\pi = 0.099, \\ \text{(II)} \quad & a_2^\pi = 0.140, a_4^\pi = 0.230, a_6^\pi = 0.180, a_8^\pi = 0.050, \end{aligned}$$

$$(III) \quad a_2^\pi = 0.160, a_4^\pi = 0.220, a_6^\pi = 0.080. \quad (31)$$

Being aware that the fitted results given in the above and [27] stand just for the “effective” values corresponding to different approximations to the Gegenbauer expansion, and in a pQCD calculation of any hard exclusive process involving a pion, the contribution of the $a_2^\pi(\mu)$ term dominates the twist-2 part, we can have consistent estimates with each other, while using these fitted DAs with and without higher-moment terms to make prediction. We would like to employ as input the parameter sets of (31).

Concerning the twist-4 DAs, there are the following parameterizations in terms of the two nonperturbative quantities δ_π^2 and ε_π :

$$\begin{aligned} \phi_{4\pi}(u) = & \frac{200}{3} \delta_\pi^2 u^2 \bar{u}^2 + 8 \delta_\pi^2 \varepsilon_\pi \{ u \bar{u} (2 + 13u \bar{u}) \\ & + 2u^3 (10 - 15u + 6u^2) \ln u + 2\bar{u}^3 (10 - 15\bar{u} + 6\bar{u}^2) \ln \bar{u} \}, \end{aligned} \quad (32)$$

$$\psi_{4\pi}(u) = \frac{20}{3} \delta_\pi^2 C_2^{\frac{1}{2}} (2u - 1), \quad (33)$$

$$\Phi_{4\pi}(\alpha_i) = 120 \delta_\pi^2 \varepsilon_\pi (\alpha_1 - \alpha_2) \alpha_1 \alpha_2 \alpha_3, \quad (34)$$

$$\Psi_{4\pi}(\alpha_i) = 30 \delta_\pi^2 (\mu) (\alpha_1 - \alpha_2) \alpha_3^2 \left[\frac{1}{3} + 2\varepsilon_\pi (1 - 2\alpha_3) \right], \quad (35)$$

$$\tilde{\Phi}_{4\pi}(\alpha_i) = -120 \delta_\pi^2 \alpha_1 \alpha_2 \alpha_3 \left[\frac{1}{3} + \varepsilon_\pi (1 - 3\alpha_3) \right], \quad (36)$$

$$\tilde{\Psi}_{4\pi}(\alpha_i) = 30 \delta_\pi^2 \alpha_3^2 (1 - \alpha_3) \left[\frac{1}{3} + 2\varepsilon_\pi (1 - 2\alpha_3) \right]. \quad (37)$$

We take the updated estimates [39] $\delta_\pi^2 = (0.18 \pm 0.06) \text{ GeV}^2$ and $\varepsilon_\pi = \frac{21}{8} \omega_{4\pi}$ ($\omega_{4\pi} = 0.2 \pm 0.1$), normalized at 1 GeV.

The remaining parameters to need pinning down include the b quark mass and decay constant of B meson. From a bottomonium sum rule calculation at four-loop precision level [40], the yielded estimate, $\overline{m}_b(\overline{m}_b) = 4.164 \pm 0.025 \text{ GeV}$, is extremely suitable as an input. As far as the latter goes, for consistency and also for narrowing down the uncertainty due to that quantity it is appropriate to take the two-point sum rule expression in terms of the b quark $\overline{\text{MS}}$ mass and with $\mathcal{O}(\alpha_s)$ accuracy, as given in [41]. In addition, we employ [42] the measurement values, $f_\pi = 130.41 \text{ MeV}$ and $m_B = 5.279 \text{ GeV}$, and two-loop running down from $\alpha_s(M_z) = 0.1185 \pm 0.0006$ for the QCD coupling constant. The factorization scale, in the light of the typical virtuality of the underlying b quark, is set at $\mu = 3.0_{-0.5}^{+1.5} \text{ GeV}$ in the case of both $f_+^{B \rightarrow \pi}(q^2)$ and $f_0^{B \rightarrow \pi}(q^2)$, while for the scale dependent quantity $f_T^{B \rightarrow \pi}(q^2)$, we estimate it at the scale $\mu = 4.8 \text{ GeV}$ for later convenience.

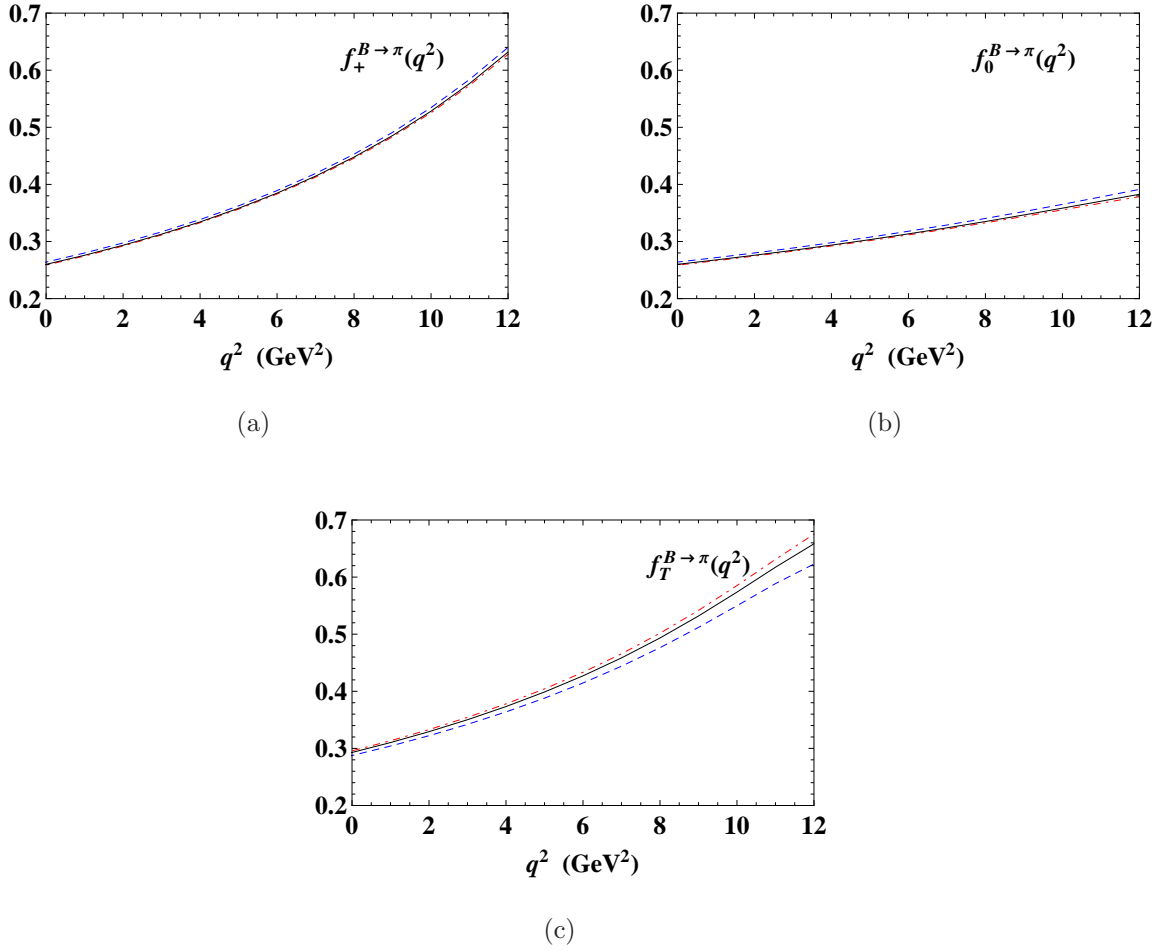


FIG. 2: Stability of the LCSRs for the $B \rightarrow \pi \ell^+ \ell^-$ form factors with respect to the variation of the Borel parameter M^2 . The solid lines indicate the central values and the regions between the red dot-dashed and blue dashed lines do the uncertainties.

As two intrinsic parameters, the effective threshold s_0 and Borel variable M^2 could be fixed in the standard procedure. Not being an universal quantity, the threshold parameter has to be independently pinned down for every sum rule we have. Taking derivative with respect to $1/M^2$ for the LCSR representations, and adjusting the yielded sum rules for B -meson mass to its measurement value, one arrives at a common result, $s_0 = (34 \pm 0.5) \text{GeV}^2$, which is below the threshold value estimated in the conventional LCSR approach, as expected. As for the Borel parameter, we choose to use, as a sum rule window shared in all these cases, the interval $M^2 = (13 - 21) \text{GeV}^2$, in which whereas the lower limit is obtained by keeping the twist-4 terms numerically reasonably small, the upper limit is determined by

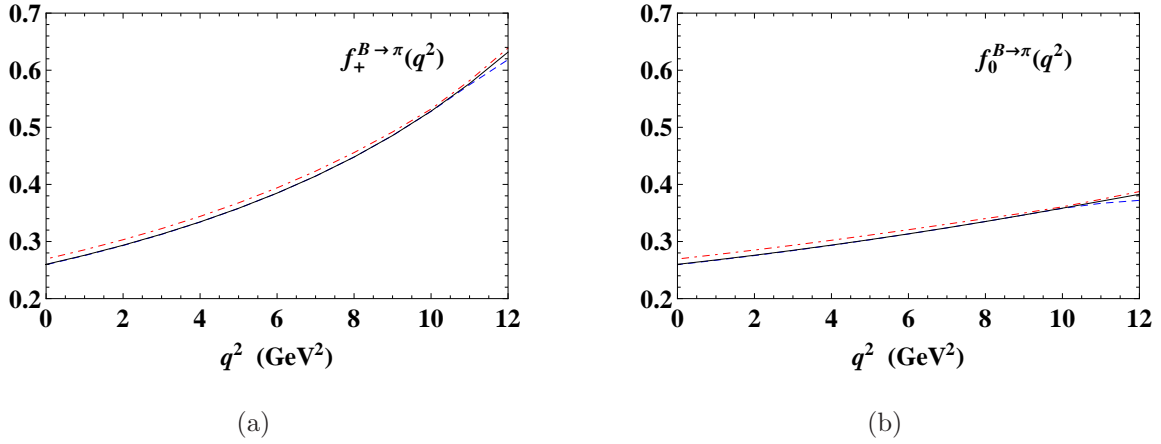


FIG. 3: Stability of the LCSRs for $f_+^{B \rightarrow \pi}(q^2)$ and $f_0^{B \rightarrow \pi}(q^2)$ with respect to the variation of the factorization scale μ . The solid lines denote the central values and the regions between the red dot-dashed and blue dashed lines do the uncertainties.

demanding that the higher-resonance and continuum contribution should not get too large.

Equipped with the specified inputs, we can assess q^2 -behavior of the $B \rightarrow \pi \ell^+ \ell^-$ form factors in the region $0 \leq q^2 \leq 12 \text{ GeV}^2$ we conservatively set. The consistency is affirmed among the calculations with the three sets of fitted moment parameters. We intend to illustrate our numerical results by focusing on the case with the parameter set (III) in (31). There is a good stability of the sum rules against the variation of the Borel parameter (see Fig.2). Moreover, as the scale parameter varies in the interval required, the sum rule results for $f_+^{B \rightarrow \pi}(q^2)$ and $f_0^{B \rightarrow \pi}(q^2)$ change by respectively less than 4.0% and 3.9% depending on q^2 , showing less sensitivity to that parameter, as expected and shown in Fig.3. Including the uncertainties achieved by adding in quadrature the separate errors due to variations of the inputs, our predictions for the form factors, which are compatible with the corresponding those using the standard LCSR approach [26, 27], are displayed in Fig.4. The results at $q^2 = 0$ read,

$$f_+^{B \rightarrow \pi}(0) = f_0^{B \rightarrow \pi}(0) = 0.260_{-0.008}^{+0.013}, \quad (38)$$

$$f_T^{B \rightarrow \pi}(0) = 0.293_{-0.014}^{+0.011}. \quad (39)$$

It is not hard to analytically continue the sum rule predictions to the high- q^2 region in

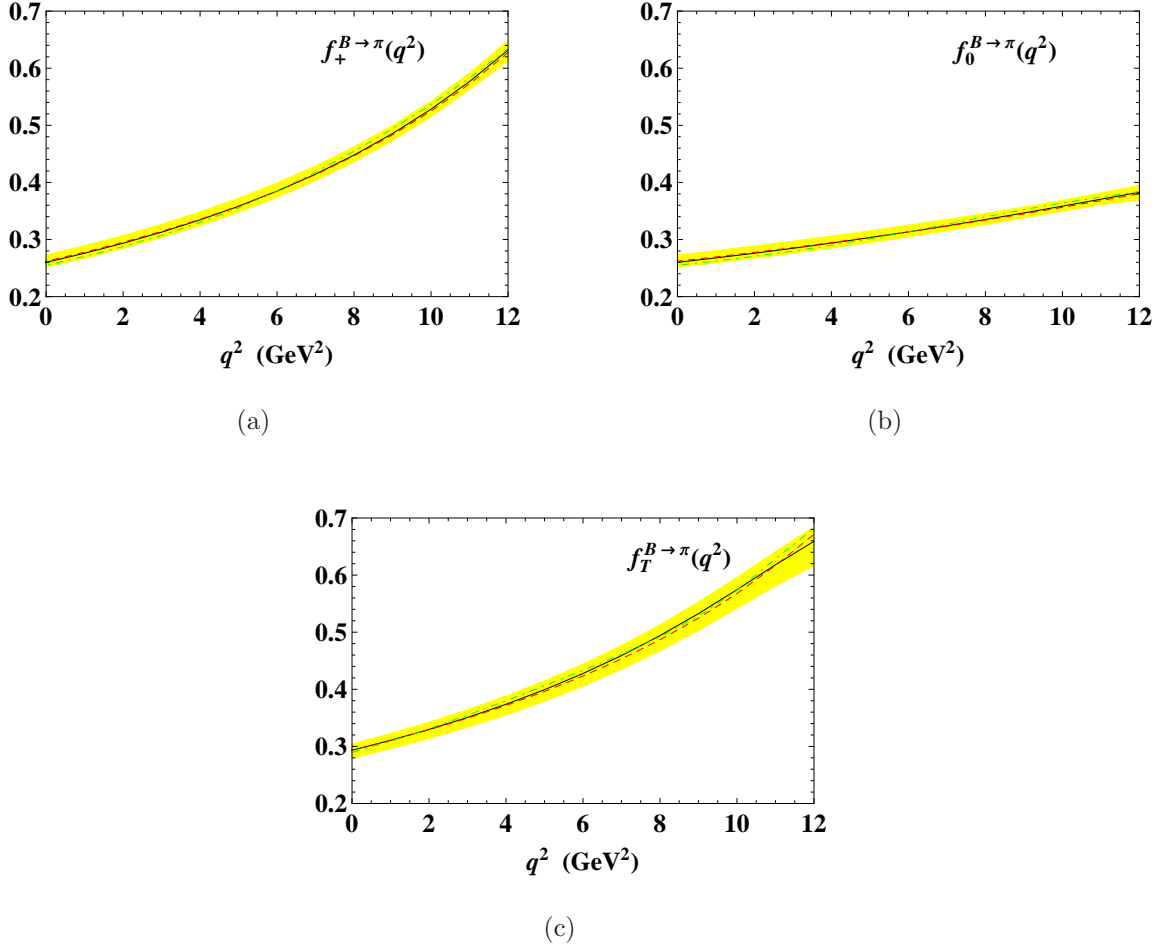


FIG. 4: q^2 -dependence of the $B \rightarrow \pi \ell^+ \ell^-$ from factors from the LCSR. The solid lines denote the central values and the yellow shadow regions show the uncertainties. The green dot-dashed (red dashed) lines denote the central values corresponding to the parameter set (I) ((II)) of (31).

a certain form factor parametrization. This has been done in [43], where the form factors obtained at $\mu = 4.8$ GeV and extrapolated analytically were used to confine the Majorana neutrino contribution to the $B \rightarrow \pi \mu^+ \mu^-$, aimed at studying the same-sign dilepton decays of B meson induced by such neutrino, a lepton flavor violating channel. From Fig.4(c) we can see, though, that when the distinct sets of moment parameter inputs are taken, the resulting shapes of the tensor form factor, despite being very close to one another, have the different trends of evolution to high q^2 . This would make uncertainty in the extrapolation large. On the other hand and more importantly, for having a reliable parametrization it is necessary to use some available estimates of these form factors at large q^2 's as an additional

bound on their behavior in the entire kinematically allowed time-like region.

III. FORM FACTOR SHAPES IN THE WHOLE KINEMATICAL REGION

Estimating the form factors in the q^2 region accessible for $B \rightarrow \pi \ell^+ \ell^-$, $0 \lesssim q^2 \leq (m_B - m_\pi)^2$ (the upper limit is about 26.4 GeV² with the measured pion mass listed in Tab. IV), we make the best of their analyticity, as well as the results based on the LCSR approach and LQCD simulation (or less model-dependent assumption). To be specific, for each form factor we fit simultaneously the theoretical predictions of these approaches to a series expansion in the mapping function $z(q^2, t_0)$, which transforms the complex q^2 -plane with a cut along the positive real axis onto the inner part of the unit circle $|z| = 1$ in the z -plane [44, 45],

$$z(q^2, t_0) = \frac{\sqrt{(m_B + m_\pi)^2 - q^2} - \sqrt{(m_B + m_\pi)^2 - t_0}}{\sqrt{(m_B + m_\pi)^2 - q^2} + \sqrt{(m_B + m_\pi)^2 - t_0}}, \quad (40)$$

where the auxiliary parameter $t_0 (< (m_B + m_\pi)^2)$ can be chosen as $t_0 = (m_B + m_\pi)^2 - 2\sqrt{m_B m_\pi} \sqrt{(m_B + m_\pi)^2 - q_0^2}$. Because the kinematical region in consideration can be mapped onto a quite small interval in the z plane by selecting optimally t_0 , an expansion around $z = 0$, with the first few terms retained, furnishes a state-of-the-art analytic approach to the form factors.

Taking into account general analytic properties of the form factors, instead of the direct expansion we adopt the Bourely-Caprini-Lellouch (BCL) versions [32, 45]:

$$f_{+(T)}^{B \rightarrow \pi}(q^2) = \frac{f_{+(T)}^{B \rightarrow \pi}(0)}{1 - q^2/m_{B^*}^2} \left\{ 1 + \sum_{k=1}^{N-1} b_k^{+(T)} \left[z(q^2, t_0)^k - z(0, t_0)^k \right. \right. \\ \left. \left. - (-1)^{N-k} \frac{k}{N} (z(q^2, t_0)^N - z(0, t_0)^N) \right] \right\}, \quad (41)$$

$$f_0^{B \rightarrow \pi}(q^2) = f_0^{B \rightarrow \pi}(0) \left\{ 1 + \sum_{k=1}^N b_k^0 (z(q^2, t_0)^k - z(0, t_0)^k) \right\}, \quad (42)$$

with the B^* -meson mass $m_{B^*} = 5.325$ GeV. Having a prefactor $\sim (1 - q^2/m_{B^*}^2)^{-1}$, the z series (41) provides an improvement to the B^* -pole dominance. For the scalar form factor there is no similar factor involved for obvious reason. The condition of unitarity does not provide, for small N , a restrictive bound on the coefficients $b_k^{+(0,T)}$, as argued in [45]. For simplicity we choose to work with a two-parameter form; that is, we truncate the expansions (41) and (42) by taking $N = 3$ and $N = 2$, respectively.

At present, the LCSR predictions for both $f_+^{B \rightarrow \pi}(q^2)$ and $f_0^{B \rightarrow \pi}(q^2)$ presented in the above section, along with the LQCD results from the HPQCD [46] and FNAL/MILC [47] collaborations are applicable to constrain the expansion parameters $b_i^{+(0)}$ ($i=1,2$). However, taking into account the fact that the b quark in the correlation function is even farther away from its mass shell at $q^2 < 0$ than at $q^2 > 0$, instead of the form factor shapes obtained in the interval $0 \leq q^2 \leq 12 \text{ GeV}^2$ we employ the LCSR results in an enlarged region $q_0^2 \leq q^2 \leq 12 \text{ GeV}^2 (q_0^2 < 0)$ in the numerical fitting, to put more restraints on the expansion coefficients. The lower limit q_0^2 is specified as $q_0^2 = -5 \text{ GeV}^2$, in order to make the light-cone OPE's have a good perturbative hierarchy. With this choice, we could fix the parameter t_0 and further the mapping function. A couple of typical mapping results are listed as follows: $q_0^2 \rightarrow |z| = 0.30$, $q^2 = 0 \rightarrow |z| = 0.26$ and $q^2 = 26.4 \text{ GeV}^2 \rightarrow |z| = 0.13$. In addition, to enhance fitting precision use should be made of the sum rule for the ratio $f_{+(0)}^{B \rightarrow \pi}(q^2)/f_{+(0)}^{B \rightarrow \pi}(0)$, in which the uncertainties due to the nonperturbative inputs cancel out in part.

The fitting is done in the standard procedure. The optimal parameter sets, yielded for each of the vector and scalar form factors by separately fitting the central values, upper and lower limits of the LCSR and LQCD results, are summarized in Tab. I. Using these as input, we get an analytical expression for describing q^2 dependence of both form factors in the kinematically allowed space-like as well as time-like regions.

TABLE I: BCL parameter sets obtained for separate estimates for the central values, upper and lower limits of the $B \rightarrow \pi$ vector (scalar) form factor as a function of q^2 .

| Parameter sets | Central values | Upper limits | Lower limits |
|--|-------------------------|------------------------|-------------------------|
| $(f_+^{B \rightarrow \pi}(0), b_1^+, b_2^+)$ | (0.260, -2.357, -1.411) | (0.273, -3.124, 1.195) | (0.252, -1.451, -4.099) |
| $(f_0^{B \rightarrow \pi}(0), b_1^0, b_2^0)$ | (0.260, -6.933, 6.635) | (0.273, -7.389, 8.351) | (0.252, -5.828, 4.600) |

For the tensor form factor, a lattice simulation has recently been performed [48], but only a preliminary result being known. To arrive at a good understanding of its behavior at high q^2 , the authors of [5] connected the $B \rightarrow \pi$ with the corresponding $B \rightarrow K$ form factors,

$$f_{+(0,T)}^{B \rightarrow \pi}(q^2) = \frac{f_{+(0,T)}^{B \rightarrow K}(q^2)}{1 + R_{+(0,T)}(q^2)}, \quad (43)$$

by invoking a $SU_F(3)$ symmetry breaking function $R_{+(0,T)}(q^2)$, and made use of the available

lattice results on both $f_{+,0,T}^{B \rightarrow K}(q^2)$ [49] and $f_{+,0}^{B \rightarrow \pi}(q^2)$ and an ansatz

$$R_T(q^2) = \frac{R_+(q^2) + R_0(q^2)}{2}, \quad (44)$$

which has been shown to be effective for low q^2 by a calculation based on heavy quark symmetry [5]. The results at eight q^2 's are demonstrated in Fig.5(c). We need to stress that they are obtained at $\mu = 4.8$ GeV, the same scale at which the low- q^2 behavior of the form factor has been predicted before by resorting to the LCSR method. Seeing that the resulting predictions may be regarded as QCD-based to a large extent, it should be in order that we use them for the parameter fitting in the absence of an available lattice estimate. Then the BCL parameter sets for the tensor form factor are accessible by doing the same as in the case of $f_{+(0)}^{B \rightarrow \pi}(q^2)$. We give the best-fitted results in Tab. II.

TABLE II: BCL parameter sets obtained for separate estimates for the central values, upper and lower limits of the $B \rightarrow \pi$ tensor form factor as a function of q^2 .

| Parameter sets | Central values | Upper limits | Lower limits |
|--|-------------------------|-------------------------|-------------------------|
| $(f_T^{B \rightarrow \pi}(0), b_1^T, b_2^T)$ | (0.293, -0.821, -2.266) | (0.304, -1.136, -1.957) | (0.279, -0.534, -2.509) |

In the fitted BCL parameterizations (41) and (42), the $B \rightarrow \pi \ell^+ \ell^-$ form factors are now understandable in the whole q^2 region. Illustrated are the resulting shapes of the vector, scalar and tensor form factors, respectively, in Figs. 5 (a), (b) and (c). At the zero recoiling point $q^2 = 26.4$ GeV², there are the following observations: $f_+^{B \rightarrow \pi}(q^2 = 26.4 \text{ GeV}^2) = 8.630$, $f_0^{B \rightarrow \pi}(q^2 = 26.4 \text{ GeV}^2) = 1.306$ and $f_T^{B \rightarrow \pi}(q^2 = 26.4 \text{ GeV}^2) = 6.203$. At this point, let us make a simple comparison between the present findings and those of [5]. The behavior we predict for $f_+^{B \rightarrow \pi}(q^2)$ resembles closely the one given in that literature through fitting the measured shape of the form factor multiplied by the CKM matrix element $|V_{ub}|$, which provides a theoretical interpretation for the observation based on data-fitting. For both $f_0^{B \rightarrow \pi}(q^2)$ and $f_T^{B \rightarrow \pi}(q^2)$, a consistent result is also observed within the estimated errors. However, whereas in [5] heavy quark symmetry is applied to constrain behavior of these two form factors in the large recoil region, here we employ for the same purpose the LCSR calculations with a chiral current correlator, from which the resulting heavy-to-light form factors could comply explicitly with the heavy quark limit behavior as predicted by soft collinear effective theory (SCET) [34], having the symmetry breaking corrections included systematically in the present estimates.

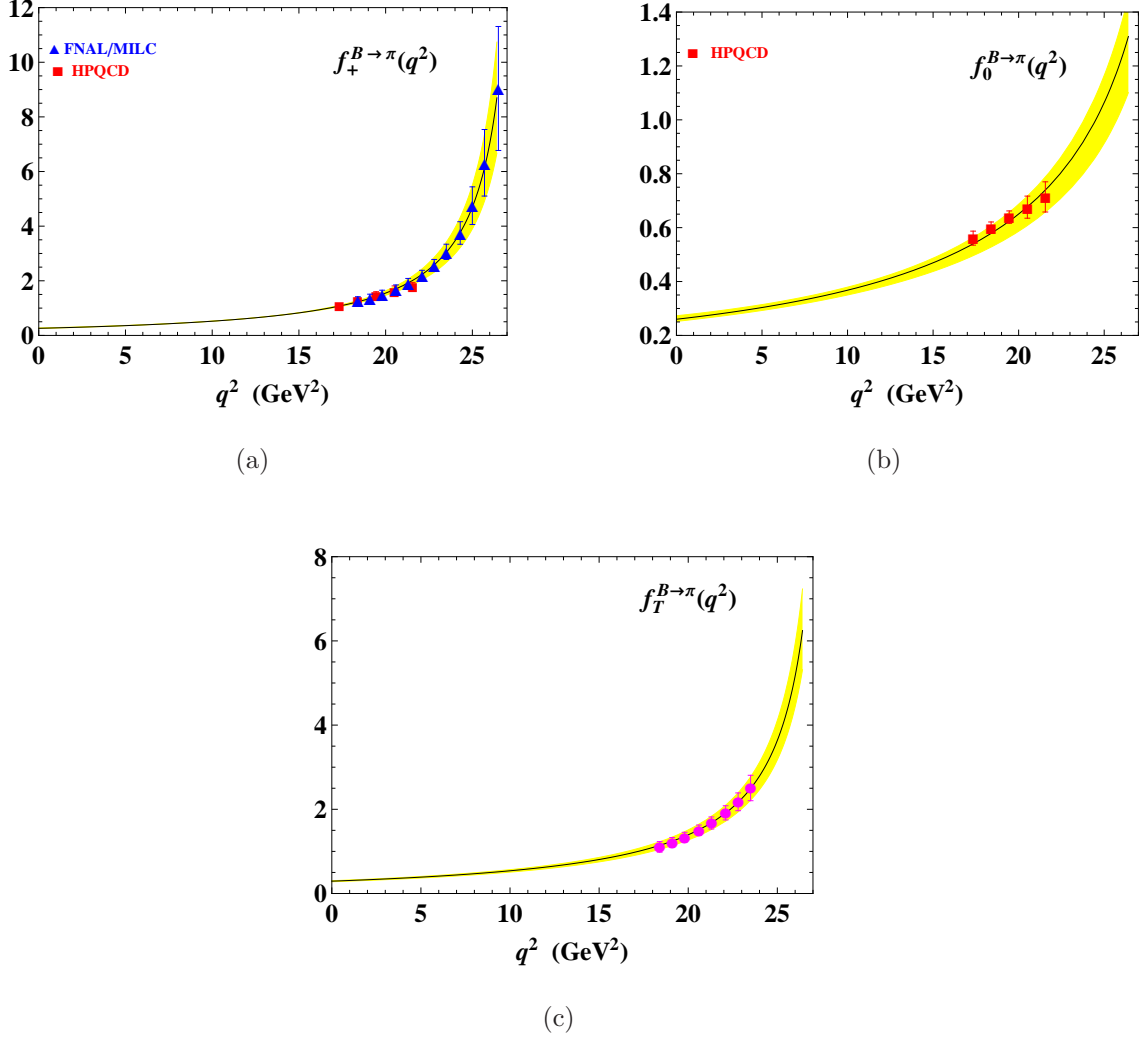


FIG. 5: Shapes of the $B \rightarrow \pi \ell^+ \ell^-$ from factors from the fitted BCL parameterizations. The solid lines represent the central values and the yellow shadow regions do the uncertainties. The magenta vertical-bars in (c) indicate the results based on both the LQCD data on the $B \rightarrow K$ tensor form factor and the $SU_F(3)$ symmetry breaking ansatz.

Certainly our theoretical predictions are available to systematically study the semileptonic $B \rightarrow \pi$ decays, including the tau lepton modes which are sensitive to the extensions of the SM with several Higgs fields. Moreover, the same approach as above applies to exploring the $B \rightarrow K \ell^+ \ell^-$ rare processes. These discussions, nevertheless, are beyond the scope of this paper.

IV. DILEPTON INVARIANT MASS DISTRIBUTIONS IN $B \rightarrow \pi\ell^+\ell^-$ AND BRANCHING RATIOS

Having in hand the $B \rightarrow \pi$ form factor parameterizations based on the available LQCD (or the quasi-model independent) and LCSR estimates obtained respectively at small and large recoil regions, we can make predictions on the decay rates and branching fractions for $B \rightarrow \pi\ell^+\ell^-$ within the naive factorization framework. The matrix elements for $B \rightarrow \pi\ell^+\ell^-$ are written as [50, 51]

$$\begin{aligned} \mathcal{M} = & \frac{G_F\alpha_{\text{em}}}{\sqrt{2}\pi} V_{tb}V_{td}^* \left[C_9^{\text{eff}}(\mu) \langle \pi(p) | \bar{d}\gamma_\mu P_L b | B(p+q) \rangle \bar{\ell}\gamma^\mu \ell \right. \\ & + C_{10}^{\text{eff}}(\mu) \langle \pi(p) | \bar{d}\gamma_\mu P_L b | B(p+q) \rangle \bar{\ell}\gamma^\mu \gamma_5 \ell \\ & \left. - 2C_7^{\text{eff}}(\mu) \frac{m_b}{q^2} \langle \pi(p) | \bar{d}i\sigma_{\mu\nu} q^\nu P_R b | B(p+q) \rangle \bar{\ell}\gamma^\mu \ell \right], \end{aligned} \quad (45)$$

based on the effective Hamiltonian responsible for the $b \rightarrow d\ell^+\ell^-$ transitions [50, 52]:

$$\mathcal{H}_{\text{eff}} = -\frac{4G_F}{\sqrt{2}} V_{tb}V_{td}^* \left[\sum_{i=1}^{10} C_i(\mu) O_i(\mu) - \lambda_u \sum_{i=1}^2 C_i(\mu) (O_i^u(\mu) - O_i(\mu)) \right]. \quad (46)$$

Here G_F and α_{em} are respectively the Fermi coupling and the fine structure constants, $P_{L,R} = (1 \mp \gamma_5)/2$, $\lambda_u (= V_{ub}V_{ud}^*/V_{tb}V_{td}^*)$ is of the standard parameterization form,

$$\lambda_u = \frac{\bar{\rho} - i\bar{\eta}}{1 - \bar{\rho} + i\bar{\eta}}, \quad (47)$$

subjected to a minor correction of $\mathcal{O}(\lambda^5)$ ($\lambda = |V_{us}|$), $O_i(\mu)$ denote the dimension-six operators with the corresponding Wilson coefficients $C_i(\mu)$, and $C_{7,9,10}^{\text{eff}}(\mu)$ stand for the effective Wilson coefficients which are particular combinations of $C_i(\mu)$ and given by [53, 54],

$$C_7^{\text{eff}} = \frac{4\pi}{\alpha_s} C_7 - \frac{1}{3} C_3 - \frac{4}{9} C_4 - \frac{20}{3} C_5 - \frac{80}{9} C_6, \quad (48)$$

$$C_9^{\text{eff}}(q^2) = \frac{4\pi}{\alpha_s} C_9 + \frac{4}{3} C_3 + \frac{64}{9} C_5 + \frac{64}{27} C_6 + Y_{\text{SD}}(q^2) + Y_{\text{LD}}(q^2), \quad (49)$$

$$C_{10}^{\text{eff}} = \frac{4\pi}{\alpha_s} C_{10}. \quad (50)$$

As shown in (49), $C_9^{\text{eff}}(q^2)$ depends on q^2 through the dynamical functions $Y_{\text{SD}}(q^2)$ and $Y_{\text{LD}}(q^2)$ parameterizing, respectively, the short- and the long-distance contributions due to the four-quark operators. The former is obtained as

$$Y_{\text{SD}}(q^2) = h(q^2, m_c) \left(\frac{4}{3} C_1 + C_2 + 6C_3 + 60C_5 \right)$$

$$\begin{aligned}
& -h(q^2, m_b) \left(\frac{7}{2}C_3 + \frac{2}{3}C_4 + 38C_5 + \frac{32}{3}C_6 \right) \\
& -h(q^2, 0) \left(\frac{1}{2}C_3 + \frac{2}{3}C_4 + 8C_5 + \frac{32}{3}C_6 \right) \\
& + \lambda_u \left(\frac{4}{3}C_1 + C_2 \right) (h(q^2, m_c) - h(q^2, 0)), \tag{51}
\end{aligned}$$

where $h(q^2, m_q)$ is the loop function dependent on the mass parameter m_q , which indicates the quark pole mass as $q = c, b$ and has been set to zero for the light quarks,

$$h(q^2, m_q) = -\frac{4}{9} \left(\ln \frac{m_q^2}{\mu^2} - \frac{2}{3} - x \right) - \frac{4}{9}(2+x)\sqrt{|x-1|} \times \begin{cases} \ln \frac{1+\sqrt{1-x}}{\sqrt{x}} - i\frac{\pi}{2}, & x \leq 1 \\ \arctan \frac{1}{\sqrt{x-1}}, & x > 1 \end{cases} \tag{52}$$

with $x = 4m_q^2/q^2$. The Wilson coefficients have been computed in next-to-next-to-leading logarithmic (NNLL) approximation through a two-loop matching of the effective with the full theory at the scale of the W -boson mass, and then evolved down to $\mu \sim m_b$ with the aid of the QCD renormalization group equations. The SM values at $\mu = 4.8\text{GeV}$ are given in Tab. III. To determine q^2 -dependence of $Y_{\text{SD}}(q^2)$, we make use of the same inputs as in [5] for the quark pole masses, $m_b = 4.91\text{ GeV}$ and $m_c = 1.77\text{ GeV}$, following from a three-loop QCD calculation [55–57] with an additional electro-weak correction [58] included. The long-distance resonance dynamics embedded in $Y_{\text{LD}}(q^2)$ is not in our consideration, because in the resonant regions such contributions can be removed experimentally and it may generally be believed, on the basis of the evaluation made for the corresponding $B \rightarrow K$ decays [18] and some indirect experimental observations, that beyond these regions the hadron resonances bring about only a moderate impact on the width.

TABLE III: SM (effective) Wilson coefficients at $\mu = 4.8\text{ GeV}$, in next-to-next-to-leading logarithmic (NNLL) approximation [54]. The function $Y(q^2)$ is defined as $Y(q^2) = \frac{4}{3}C_3 + \frac{64}{9}C_5 + \frac{64}{27}C_6 + Y_{\text{SD}}(q^2) + Y_{\text{LD}}(q^2)$.

| C_1 | C_2 | C_3 | C_4 | C_5 | C_6 | C_7^{eff} | $C_9^{\text{eff}} - Y(q^2)$ | C_{10}^{eff} |
|--------|-------|--------|--------|-------|-------|--------------------|-----------------------------|-----------------------|
| -0.257 | 1.009 | -0.005 | -0.078 | 0.000 | 0.001 | -0.304 | 4.211 | -4.103 |

For the $b \rightarrow d$ hadronic matrix elements entering (45) using their standard parameterization forms (1), we get the differential branching ratios for, say, the charged decay models

$B^- \rightarrow \pi^- \ell^+ \ell^-$,

$$\frac{d\mathcal{B}(B^- \rightarrow \pi^- \ell^+ \ell^-)}{dq^2} = \frac{G_F^2 \alpha_{\text{em}}^2 \tau_B}{2^{10} \pi^5 m_B^3} |V_{tb} V_{td}^*|^2 \sqrt{\lambda(q^2)} \left(1 - \frac{4m_\ell^2}{q^2}\right) \sigma(q^2), \quad (53)$$

where $\tau_B = 1.638 \pm 0.004$ ps denotes the B meson lifetime, m_ℓ the lepton mass, $\lambda(q^2) = (m_B^2 + m_\pi^2 - q^2)^2 - 4m_B^2 m_\pi^2$, and

$$\begin{aligned} \sigma(q^2) = & \frac{2}{3} \lambda(q^2) \left[\left(1 + \frac{2m_\ell^2}{q^2}\right) \left| C_9^{\text{eff}}(q^2) f_+^{B \rightarrow \pi}(q^2) + \frac{2m_b}{m_B + m_\pi} C_7^{\text{eff}} f_T^{B \rightarrow \pi}(q^2) \right|^2 \right. \\ & \left. + \left(1 - \frac{4m_\ell^2}{q^2}\right) |C_{10}^{\text{eff}} f_+^{B \rightarrow \pi}(q^2)|^2 \right] + \frac{4m_\ell^2}{q^2} (m_B^2 - m_\pi^2)^2 |C_{10}^{\text{eff}} f_0^{B \rightarrow \pi}(q^2)|^2, \quad (54) \end{aligned}$$

of which the last term on the right-hand side includes a factor of m_ℓ^2 which is numerically close to zero for $\ell = e, \mu$, so that the scalar form factor plays a negligible role for the decays with a dielectron or dimuon in the final state.

TABLE IV: Some of the parameter inputs used in the numerical analysis [42].

| | | | |
|---------------|---|--------------|-------------------|
| α_{em} | 1/137 | $\bar{\eta}$ | 0.354 ± 0.015 |
| G_F | $1.16638 \times 10^{-5} \text{ GeV}^{-2}$ | m_e | 0.511 MeV |
| $ V_{tb} $ | 0.99914 | m_μ | 0.106 GeV |
| $ V_{td} $ | $0.00886^{+0.00033}_{-0.00032}$ | m_τ | 1.777 GeV |
| $\bar{\rho}$ | 0.124 ± 0.024 | m_π | 0.13957 GeV |

TABLE V: Summary of the SM predictions (in 10^{-8}) for the branching ratios for $B^- \rightarrow \pi^- \ell^+ \ell^-$ ($\ell = e, \mu, \tau$) in naive factorization.

| Modes | LHCb experiment[1] | Theoretical predictions | | | | |
|---------------------------------------|-----------------------|---------------------------|-----------------|------------------------|------------------------|-----------------|
| | | This work | [3] | [4] | [5] | [6] |
| $B^- \rightarrow \pi^- e^+ e^-$ | -- | $2.263^{+0.227}_{-0.192}$ | 2.03 ± 0.23 | $1.95^{+0.61}_{-0.48}$ | -- | -- |
| $B^- \rightarrow \pi^- \mu^+ \mu^-$ | $2.3 \pm 0.6 \pm 0.1$ | $2.259^{+0.226}_{-0.191}$ | 2.03 ± 0.23 | $1.95^{+0.61}_{-0.48}$ | $1.88^{+0.32}_{-0.21}$ | 2.0 ± 0.2 |
| $B^- \rightarrow \pi^- \tau^+ \tau^-$ | -- | $1.017^{+0.118}_{-0.139}$ | -- | $0.60^{+0.18}_{-0.14}$ | -- | 0.70 ± 0.07 |

Neglecting the isospin-symmetry breaking effect, in the following numerical discussion we take the $B^- \rightarrow \pi^- \ell^+ \ell^-$ modes as an illustrate example. In Fig.6, shown are the dilepton

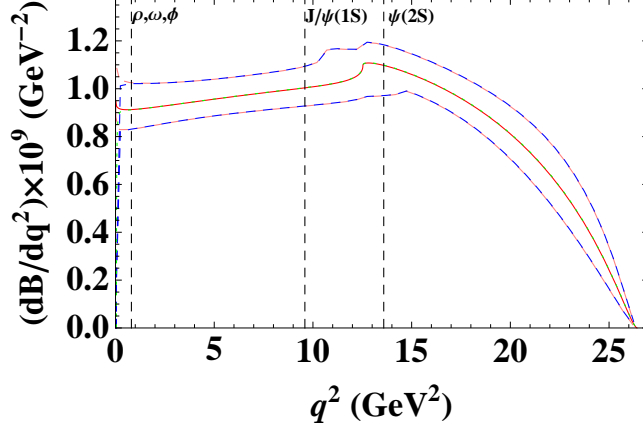


FIG. 6: Invariant mass distributions in $B^- \rightarrow \pi^- e^+ e^-$ and $B^- \rightarrow \pi^- \mu^+ \mu^-$, with the central values denoted by respectively the red solid and green dotted lines, and the uncertainty bounds shown by respectively the pink dashed and blue dashed lines.

invariant mass distributions in $B^- \rightarrow \pi^- \ell^+ \ell^-$ ($\ell = e, \mu$) obtained in the corresponding kinematically accessible regions $4m_\ell^2 \leq q^2 \leq (m_B - m_\pi)^2$ with the predicted form factor shapes together with the parameter inputs listed in Tab. IV, which coincide to a reasonably large extent with each other. A similar distribution is given in [5], however in the central value there exists about a -10% to -15% deviation from the present estimates, depending on q^2 . Unfortunately, no experimental measurement is available to make comparison. The branching ratios are estimated at:

$$\mathcal{B}(B^- \rightarrow \pi^- e^+ e^-) = (2.263_{-0.161}^{+0.172} |_{\text{CKM}} \quad +0.143_{-0.095} |_{\text{FF}} \quad +0.040_{-0.044}) \times 10^{-8}, \quad (55)$$

$$\mathcal{B}(B^- \rightarrow \pi^- \mu^+ \mu^-) = (2.259_{-0.160}^{+0.172} |_{\text{CKM}} \quad +0.141_{-0.094} |_{\text{FF}} \quad +0.040_{-0.044}) \times 10^{-8}, \quad (56)$$

where the uncertainties originating from the related CKM matrix elements and the form factors are separately given. The resulting prediction (56) can be well accommodated by the experimental result by the LHCb collaboration, but has a slightly larger central value than those reported in [3–6] (see Tab.V). Also, it is of specific experimental interest to compute the partial branching ratios in some chosen q^2 intervals. In Tab.VI the results yielded for $B^- \rightarrow \pi^- \mu^+ \mu^-$ are summarized and some of them are compared with the predictions in [5] and in the context of QCDF [7].

It is absolutely essential to investigate the $B^- \rightarrow \pi^- \tau^+ \tau^-$ decay, which albeit is difficult to detect due to the tau lepton's short lifetime. Other than the dielectronic and dimuonic

TABLE VI: Theoretical predictions for the $B^- \rightarrow \pi^- \mu^+ \mu^-$ partial branching ratios in some chosen q^2 intervals (in 10^{-8}).

| $[q_{min}^2, q_{max}^2]$ | $\mathcal{B}(q_{min}^2 \leq q^2 \leq q_{max}^2)$ | | |
|--------------------------|--|------------------------|------------------------|
| | This work | [5] | [7] |
| [0.05, 2.0] | $0.177^{+0.021}_{-0.015}$ | $0.15^{+0.03}_{-0.02}$ | -- |
| [1.0, 2.0] | $0.092^{+0.010}_{-0.008}$ | $0.08^{+0.01}_{-0.01}$ | -- |
| [2.0, 4.3] | $0.215^{+0.021}_{-0.017}$ | $0.19^{+0.03}_{-0.02}$ | -- |
| [4.3, 8.68] | $0.426^{+0.037}_{-0.031}$ | $0.37^{+0.06}_{-0.04}$ | -- |
| [0.05, 8.0] | $0.751^{+0.070}_{-0.057}$ | $0.66^{+0.10}_{-0.07}$ | -- |
| [1.0, 6.0] | $0.470^{+0.045}_{-0.036}$ | -- | $0.44^{+0.06}_{-0.05}$ |
| [2.0, 6.0] | $0.378^{+0.035}_{-0.028}$ | -- | $0.36^{+0.05}_{-0.04}$ |
| [1.0, 8.0] | $0.666^{+0.060}_{-0.050}$ | $0.58^{+0.09}_{-0.06}$ | $0.63^{+0.09}_{-0.07}$ |
| [10.09, 12.86] | $0.288^{+0.033}_{-0.025}$ | $0.25^{+0.04}_{-0.03}$ | -- |
| [14.18, 16.0] | $0.192^{+0.016}_{-0.014}$ | $0.15^{+0.03}_{-0.02}$ | -- |
| [16.0, 18.0] | $0.197^{+0.018}_{-0.016}$ | $0.15^{+0.03}_{-0.02}$ | -- |
| [18.0, 22.0] | $0.322^{+0.046}_{-0.042}$ | $0.25^{+0.04}_{-0.03}$ | -- |
| [22.0, 26.4] | $0.155^{+0.046}_{-0.039}$ | $0.13^{+0.02}_{-0.02}$ | -- |
| [12.0, 14.0] | $0.218^{+0.018}_{-0.025}$ | -- | -- |
| [14.0, 16.0] | $0.212^{+0.017}_{-0.016}$ | -- | -- |
| [16.0, 18.0] | $0.197^{+0.018}_{-0.016}$ | -- | -- |
| [18.0, 20.0] | $0.176^{+0.021}_{-0.019}$ | -- | -- |
| [20.0, 22.0] | $0.147^{+0.025}_{-0.023}$ | -- | -- |
| [22.0, 24.0] | $0.106^{+0.027}_{-0.024}$ | -- | -- |
| [24.0, 26.4] | $0.049^{+0.019}_{-0.016}$ | -- | -- |

decays, this type of modes are made depend strongly on the scalar form factor and have a much narrower kinematical region by the large tau lepton mass. Hence they as well as $B \rightarrow \pi$ semileptonic decays into a tau lepton could be used to examine our prediction for the form factor in intermediate and large q^2 region, under the prerequisite, of course, that all possible new physics effects on these modes are negligibly small. We have the invariant

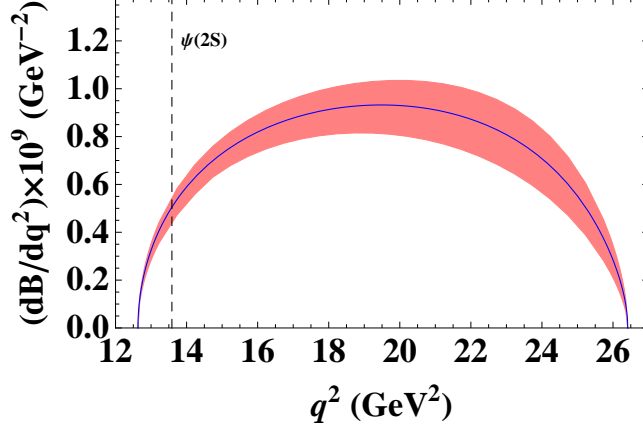


FIG. 7: Invariant mass distribution in $B^- \rightarrow \pi^- \tau^+ \tau^-$. The blue solid line indicates the central values and the pink shadow region does the uncertainties.

TABLE VII: Theoretical predictions for the $B^- \rightarrow \pi^- \tau^+ \tau^-$ partial branching ratios in some chosen q^2 intervals (in 10^{-8}).

| $[q_{min}^2, q_{max}^2]$ | $\mathcal{B}(q_{min}^2 \leq q^2 \leq q_{max}^2)$ |
|--------------------------|--|
| [12.6, 14.0] | $0.056^{+0.005}_{-0.007}$ |
| [14.0, 16.0] | $0.144^{+0.012}_{-0.015}$ |
| [16.0, 18.0] | $0.175^{+0.016}_{-0.019}$ |
| [18.0, 20.0] | $0.185^{+0.019}_{-0.023}$ |
| [20.0, 22.0] | $0.182^{+0.023}_{-0.027}$ |
| [22.0, 24.0] | $0.160^{+0.025}_{-0.029}$ |
| [24.0, 26.4] | $0.114^{+0.022}_{-0.026}$ |

mass distribution shown in Fig.7 and the branching ratio,

$$\mathcal{B}(B^- \rightarrow \pi^- \tau^+ \tau^-) = (1.017^{+0.077}_{-0.072}|_{\text{CKM}} \quad {}^{+0.090}_{-0.119}|_{\text{FF}} \quad {}^{+0.004}_{-0.006}) \times 10^{-8}. \quad (57)$$

Compared with the previous studies using the pQCD method [4] and the relativistic quark model [6], an increase of one order of magnitude is here observed in the branching ratio, as shown in Tab.V. This difference is mainly caused by the difference in the shape of the scalar form factor used as input. The partial branching ratios assessed in several q^2 bins are collected in Tab.VII.

It is realistic to expect very soon the release of available LQCD data on the $f_T^{B \rightarrow \pi}(q^2)$ form

factor. Then we can have an updated result for its q^2 behavior and thus for the observables, which, however, is not expected to substantially improve the present estimates.

V. SUMMARY

We have reported a novel approach to the $B \rightarrow \pi \ell^+ \ell^-$ form factors in the whole semileptonic region, which combines the LCSR method, LQCD simulation, $SU_F(3)$ symmetry breaking analysis and form factor analyticity, and applied the resulting form factor predictions to estimate several important observables of these rare modes in naive factorization.

To twist-2 NLO accuracy and with the $\overline{\text{MS}}$ mass for the underlying b quark, the shapes of the form factors in the region $0 \leq q^2 \leq 12 \text{ GeV}^2$ are estimated in the LCSR approach with a chiral current correlator, and a result free of pollution by twist-3 is obtained. We further investigate their behavior in the entire kinematically accessible region. For both vector and scalar form factors, a simultaneous fit to a two-parameter BCL series is carried out of the sum rule results in an enlarged q^2 region and the corresponding LQCD ones available at some high q^2 's. Given lack of available LQCD data on the tensor form factor, as a similar procedure is applied for an all-around understanding of its behavior we use as a constraint condition at high q^2 the LQCD prediction for the corresponding $B \rightarrow K$ form factor in conjunction with a $SU_F(3)$ symmetry breaking ansatz. With the fitted parameterizations, we make a prediction for the dilepton invariant mass spectra and branching ratios for $B \rightarrow \pi \ell^+ \ell^-$, by taking as an example the $B^- \rightarrow \pi^-$ charged decay modes. For the dielectron and dimuon modes, a branching ratio in good agreement with the experimental measurement is obtained as, $\mathcal{B}(B^- \rightarrow \pi^- e^+ e^-) = (2.263_{-0.192}^{+0.227}) \times 10^{-8}$ and $\mathcal{B}(B^- \rightarrow \pi^- \mu^+ \mu^-) = (2.259_{-0.191}^{+0.226}) \times 10^{-8}$. Consequently a more stringent constraint than what have been achieved before is imposed on the possible new physics contribution. In contrast, the corresponding observation made for the ditau mode is $\mathcal{B}(B^- \rightarrow \pi^- \tau^+ \tau^-) = (1.017_{-0.139}^{+0.118}) \times 10^{-8}$, which turns out to be one order of magnitude larger than the previous predictions based on the form factor calculations by two other approaches. We present also an assessment of the partial branching ratios in some chosen q^2 bins, which can be confronted with the future experimental data, along with the resulting invariant mass distributions.

On the ground of the present findings and experimental measurement for $B \rightarrow \pi \mu^+ \mu^-$, it seems that there is less room left for physics beyond the SM in the $B \rightarrow \pi$ dileptonic

modes. However, it is still too early to draw any final conclusion, because possible new physics, if exists, would be expected to manifest itself through some other observables, such as the CP and the forward-backward asymmetries. Whereas in the SM a trustworthy result for the CP asymmetry in the charged decay modes is difficult to achieve due to our limited understanding of the two main sources of uncertainty, the long-distance function $Y_{LD}(q^2)$ and weak-annihilation, the forward-backward asymmetry is precisely zero and thereby its non-zero measurement would be a clean signal of new effective couplings out of the SM scope.

ACKNOWLEDGEMENTS

N. Zhu is indebted to Dr. Y. -M. Wang for enormously helpful discussion in the numerical analysis of the sum rules. This work is in part supported by the National Science Foundation of China (Key Program) under Grant Nos. 11235005, 11325525 and 11275114.

-
- [1] LHCb Collaboration, *JHEP* **12** (2012) 125 [arXiv:1210.2645 [hep-ex]].
- [2] F. Krüger and L. M. Sehgal, *Phys. Rev. D* **56** (1997) 5452, Erratum-ibid. *D* **60** (1999) 099905 [arXiv:hep-ph/9706247].
- [3] J. J. Wang, R. M. Wang, Y. G. Xu and Y. D. Yang, *Phys. Rev. D* **77** (2008) 014017 [arXiv:0711.0321 [hep-ph]].
- [4] W. F. Wang and Z. J. Xiao, *Phys. Rev. D* **86** (2012) 114025 [arXiv:1207.0265 [hep-ph]].
- [5] A. Ali, A. Y. Parkhomenko and A. V. Rusov, *Phys. Rev. D* **89** (2014) 094021 [arXiv:1312.2523 [hep-ph]].
- [6] R. N. Faustov and V. O. Galkin, *Eur. Phys. J. C* **74** (2014) 2911 [arXiv:1403.4466 [hep-ph]].
- [7] W. S. Hou, M. Kohda and F. R. Xu, *Phys. Rev. D* **90** (2014) 013002 [arXiv:1403.7410v2 [hep-ph]].
- [8] T. M. Aliev and M. Savci, *Phys. Rev. D* **60** (1999) 014005 [arXiv:hep-ph/9812272].
- [9] S. R. Choudhury and N. Gaur, *Phys. Rev. D* **66** (2002) 094015 [arXiv:hep-ph/0206128].
- [10] H. Z. Song, L. X. Lu and G. R. Lu, *Commun. Theor. Phys.* **50** (2008) 696 [DOI: 10.1088/0253-6102/50/3/35].
- [11] M. Beneke, G. Buchalla, M. Neubert and C. T. Sachrajda, *Phys. Rev. Lett.* **83** (1999) 1914 [arXiv:hep-ph/9905312].
- [12] M. Beneke, G. Buchalla, M. Neubert and C. T. Sachrajda, *Nucl. Phys. B* **591** (2000) 313 [arXiv:hep-ph/0006124].
- [13] M. Beneke and T. Feldmann, *Nucl. Phys. B* **592** (2001) 3 [arXiv:hep-ph/0008255].
- [14] M. Beneke, T. Feldmann and D. Seidel, *Nucl. Phys. B* **612** (2001) 25 [arXiv:hep-ph/0106067].
- [15] A. Ali and A. Y. Parkhomenko, *Eur. Phys. J. C* **23** (2002) 89 [arXiv:hep-ph/0105302].
- [16] S. W. Bosch and G. Buchalla, *Nucl. Phys. B* **621** (2002) 459 [arXiv:hep-ph/0106081].
- [17] M. Beneke, T. Feldmann and D. Seidel, *Eur. Phys. J. C* **41** (2005) 173 [arXiv:hep-ph/0412400].
- [18] A. Khodjamirian, T. Mannel and Y. M. Wang, *JHEP* **1302** (2013) 010 [arXiv:1211.0234 [hep-ph]].
- [19] I. Balitsky, V. M. Braun and A. Kolesnichenko, *Nucl. Phys. B* **312** (1989) 509.
- [20] V. L. Chernyak and I. R. Zhitnitsky, *Nucl. Phys. B* **345** (1990) 137 [DOI: 10.1016/0550-3213(90)90612-H].

- [21] H. N. Li, Y. L. Shen and Y. M. Wang, Phys. Rev. D **85** (2012) 074004 [arXiv:1201.5066 [hep-ph]].
- [22] P. Ball and R. Zwicky, Phys. Rev. D **71** (2005) 014015 [arXiv:0406232].
- [23] Particle Data Group Collaboration, Phys. Rev. D **86** (2012) 010001 [DOI: 10.1103/PhysRevD.86.010001].
- [24] Z. H. Li, N. Zhu, X. J. Fan and T. Huang, JHEP **05** (2012) 160 [arXiv:1206.0091 [hep-ph]].
- [25] A. Bharucha, JHEP **05** (2012) 092 [arXiv:1203.1359 [hep-ph]].
- [26] G. Duplancic, A. Khodjamirian, T. Mannel, B. Melic and N. Offen, JHEP **0804** (2008) 014 [arXiv:0801.1796 [hep-ph]].
- [27] A. Khodjamirian, T. Mannel, N. Offen and Y. M. Wang, Phys. Rev. D **83** (2011) 094031 [arXiv:1103.2655 [hep-ph]].
- [28] T. Huang, Z. H. Li and X. Y. Wu, Phys. Rev. D **63** (2001) 094001 [DOI: 10.1103/PhysRevD.63.094001].
- [29] P. Ball, Phys. Lett. B **641** (2006) 50 [arXiv:hep-ph/0608116].
- [30] P. Ball and A. N. Talbot, JHEP **0506** (2005) 063 [arXiv:hep-ph/0502115].
- [31] P. Ball and R. Zwicky, Phys. Lett. B **625** (2005) 225, [arXiv:hep-ph/0507076].
- [32] A. Khodjamirian, C. Klein, T. Mannel and N. Offen, Phys. Rev. D **80** (2009) 114005 [arXiv:0907.2842 [hep-ph]].
- [33] J. Charles, A. Le Yaouanc, L. Oliver, O. Pene, J. C. Raynal, Phys. Rev. D **60** (1999) 014001 [arXiv:hep-ph/9812358].
- [34] C. W. Bauer, S. Fleming, D. Pirjol and I. W. Stewart, Phys. Rev. D **63** (2001) 114020 [arXiv:hep-ph/0011336].
- [35] T. Huang, X. G. Wu and T. Zhong, Chin. Phys. Lett. **30** (2013) 041201 [arXiv:1303.2301 [hep-ph]].
- [36] T. Huang, T. Zhong and X. G. Wu, Phys. Rev. D **88** (2013) 034013 [arXiv:1305.7391 [hep-ph]].
- [37] X. G. Wu and T. Huang, Phys. Rev. D **79** (2009) 034013. [arXiv:0901.2636 [hep-ph]].
- [38] S. S. Agaev, V. M. Braun, N. Offen and F. A. Porkert, Phys. Rev. D **83** (2011) 054020 [arXiv:1012.4671 [hep-ph]].
- [39] P. Ball, V. M. Braun and A. Lenz, JHEP **0605** (2006) 004 [arXiv:hep-ph/0603063].
- [40] J. H. Kuehn, M. Steinhauser and C. Sturm, Nucl. Phys. B **778** (2007) 192 [arXiv:hep-ph/0702103].

- [41] M. Jamin and B. O. Lange, Phys. Rev. D **65** (2002) 056005 [arXiv:hep-ph/0108135].
- [42] Particle Data Group Collaboration, Chin. Phys. C **38** (2014) 090001 [DOI: 10.1088/1674-1137/38/9/090001].
- [43] Y. Wang, S. S. Bao, Z. H. Li, N. Zhu and Z. G. Si, Phys. Lett. B **736** (2014) 428 [arXiv:1407.2468 [hep-ph]].
- [44] C. G. Boyd, B. Grinstein and R. F. Lebed, Phys. Rev. Lett. **74** (1995) 4603 [arXiv:hep-ph/9412324].
- [45] C. Bourrely, I. Caprini and L. Lellouch, Phys. Rev. D **79** (2009) 013008; Erratum-ibid. D **82** (2010) 099902 [arXiv:0807.2722 [hep-ph]].
- [46] E. Gulez, A. Gray, M. Wingate, C. T. H. Davies, G. P. Lepage and J. Shigemitsu, Phys. Rev. D **73** (2006) 074502, Erratum-ibid. D **75** (2007) 119906 [arXiv:hep-lat/0601021].
- [47] J. A. Bailey et al, Phys. Rev. D **79** (2009) 054507 [arXiv:0811.3640 [hep-lat]].
- [48] C. M. Bouchard, G. P. Lepage, C. J. Monahan, H. Na and J. Shigemitsu, [arXiv:1310.3207 [hep-lat]].
- [49] C. Bouchard, G. P. Lepage, C. Monahan, H. Na and J. Shigemitsu, Phys. Rev. D **88** (2013) 054509 [arXiv:1306.2384 [hep-lat]].
- [50] A. J. Buras and M. Muenz, Phys. Rev. D **52** (1995) 186 [arXiv:hep-ph/9501281 [hep-ph]].
- [51] F. Krüger and L. M. Sehgal, Phys. Rev. D **55** (1997) 2799 [arXiv:hep-ph/9608361].
- [52] G. Buchalla, A. J. Buras and M. E. Lautenbacher, Rev. Mod. Phys. **68** (1996) 1125 [arXiv:hep-ph/9512380].
- [53] A. J. Buras, M. Misiak, M. Muenz and S. Pokorski, Nucl. Phys. B **424** (1994) 374 [arXiv:hep-ph/9311345].
- [54] W. Altmannshofer, P. Ball, A. Bharucha, A. J. Buras, D. M. Straub and M. Wick, JHEP **0901** (2009) 019 [arXiv:0811.1214 [hep-ph]].
- [55] K. Chetyrkin and M. Steinhauser, Phys. Rev. Lett. **83** (1999) 4001 [arXiv:hep-ph/9907509].
- [56] K. Chetyrkin and M. Steinhauser, Nucl. Phys. B **573** (2000) 617 [arXiv:hep-ph/9911434].
- [57] K. Melnikov and T. V. Ritbergen, Phys. Lett. B **482** (2000) 99 [arXiv:hep-ph/9912391].
- [58] Z. Z. Xing, H. Zhang, and S. Zhou, Phys. Rev. D **77** (2008) 113016 [arXiv:0712.1419 [hep-ph]].